Applications of AI to CT Image Formation

Marc Kachelrieß

German Cancer Research Center (DKFZ)

Heidelberg, Germany

www.dkfz.de/ct

DEUTSCHES KREBSFORSCHUNGSZENTRUM IN DER HELMHOLTZ-GEMEINSCHAFT

Part 1:

Making up Data

MAR Example

- Deep CNN-driven patch-based combination of the advantages of several MAR methods trained on simulated artifacts

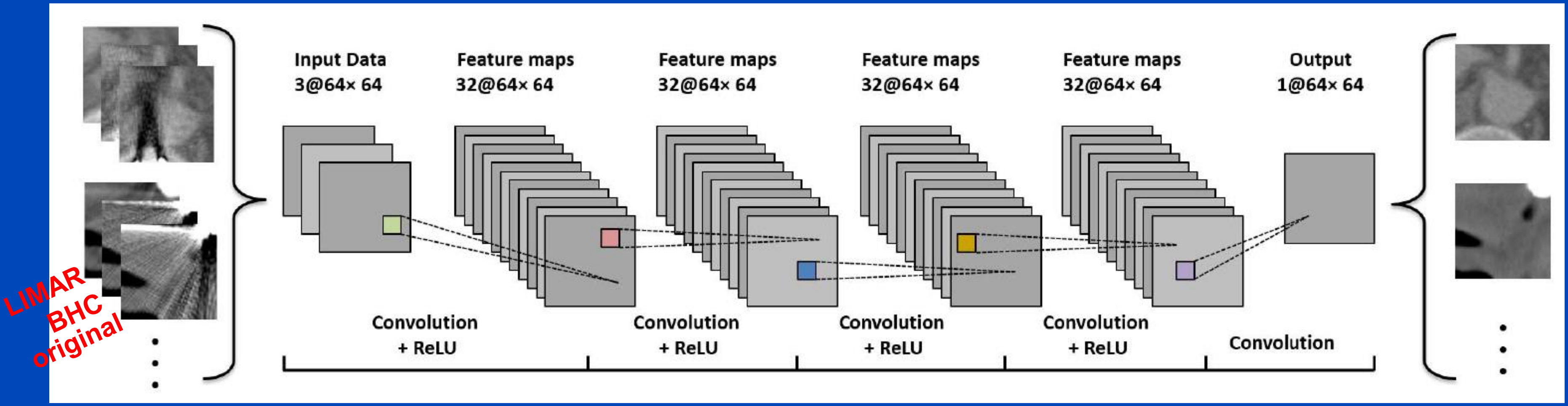

- followed by segmentation into tissue classes
- followed by forward projection of the CNN prior and replacement of metal areas of the original sinogram
- followed by reconstruction

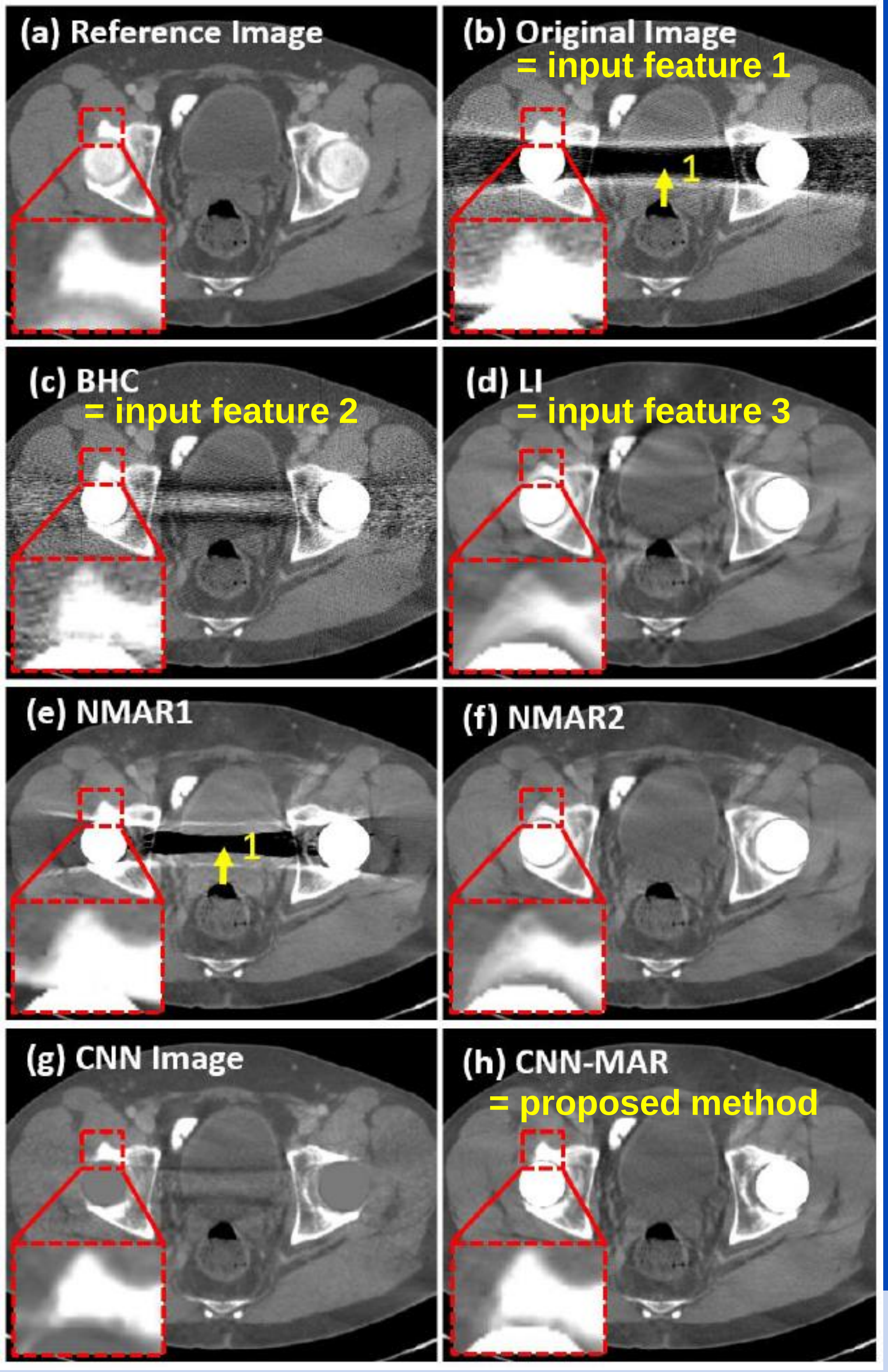
(a) Reference Image
(b) Original Image
= input feature 1
1
(c) BHC
= input feature 2
(d) LI
= input feature 3
(e) NMAR1
1
(f) NMAR2
(g) CNN Image
(h) CNN-MAR
= proposed method

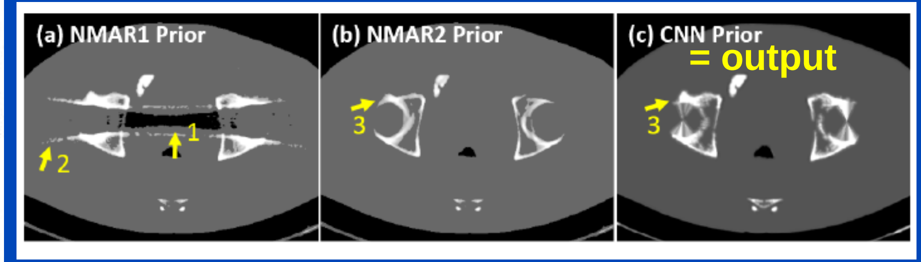
(a) NMAR1 Prior
1
2
(b) NMAR2 Prior
3
(c) CNN Prior
= output
3

Sparse View Restoration Example

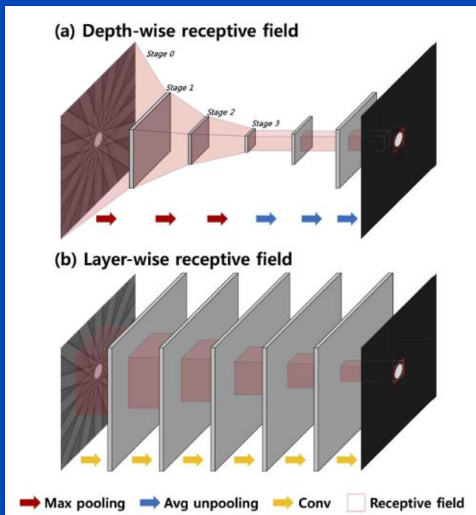

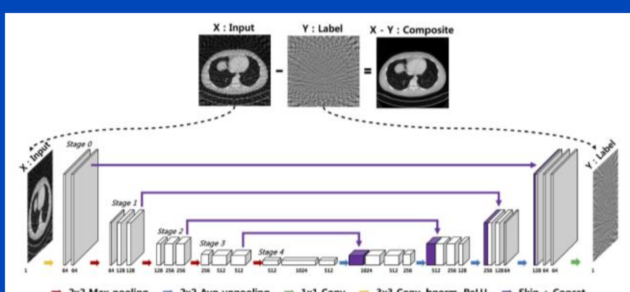

Figure 1. The proposed deep residual learning architecture for sparse view CT reconstruction.

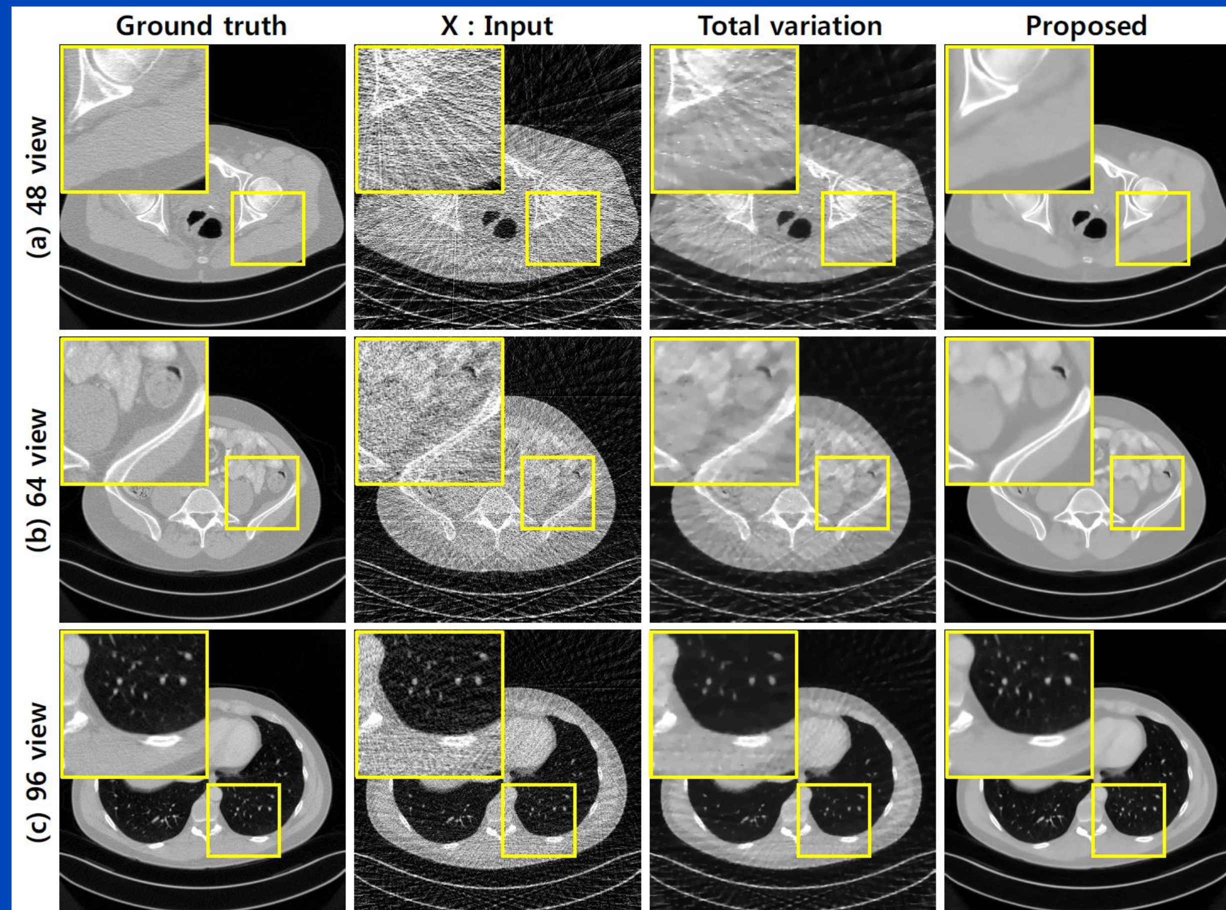

Yo Seob Han, Jaejun Yoo and Jong Chul Ye. Deep Residual Learning for Compressed Sensing CT Reconstruction via Persistent Homology Analysis. ArXiv 2016.

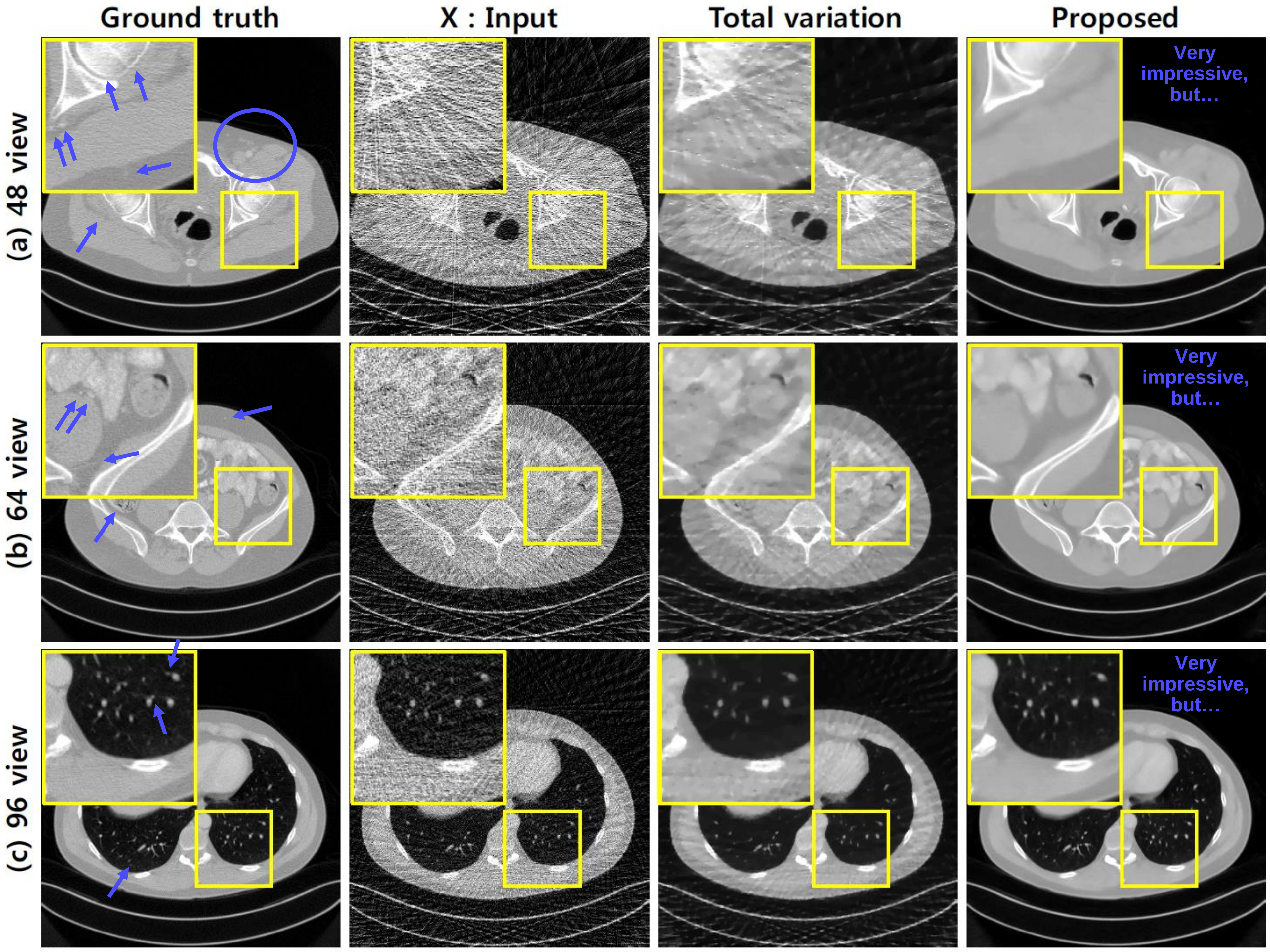

Ground truth
X : Input
Total variation
Proposed
(a) 48 view
(b) 64 view
(c) 96 view
Very impressive, but…
Very impressive, but…
Very impressive, but…

Part 2:

Noise Reduction

Canon's AiCE

- Advanced intelligent Clear-IQ Engine (AiCE)
- Trained to restore low-dose CT data to match the properties of FIRST, the model-based IR of Canon.
- FIRST is applied to high-dose CT images to obtain a high fidelity training target

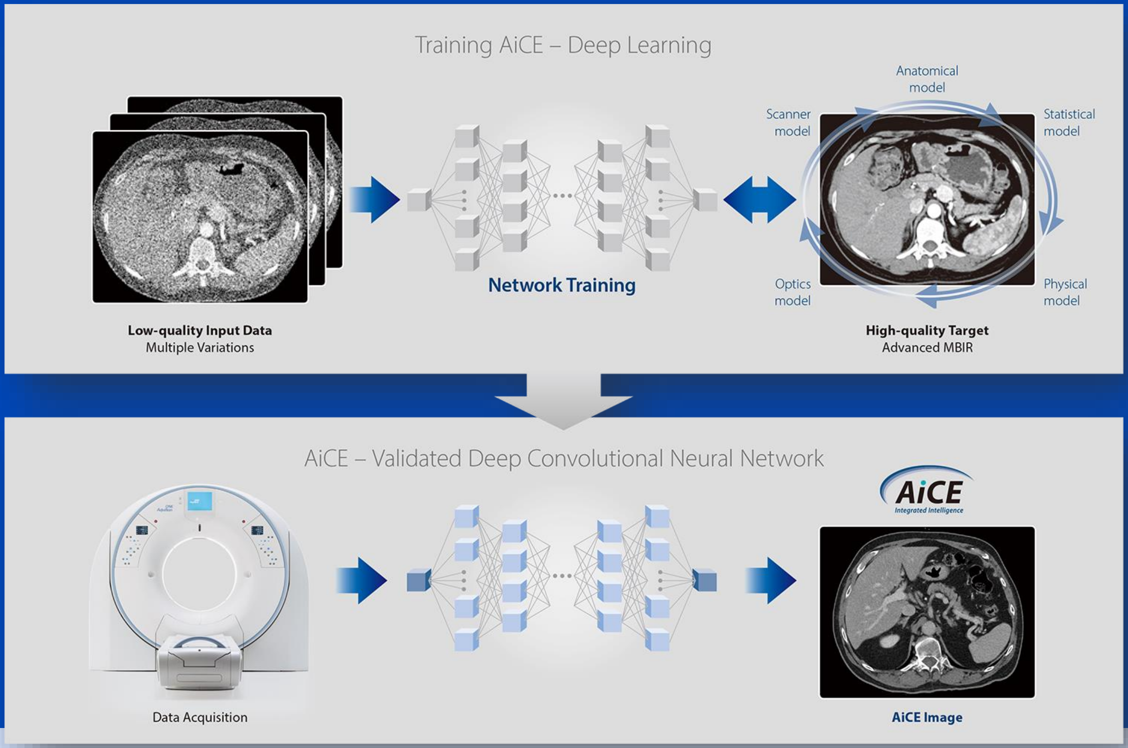

Information taken from https://global.medical.canon/products/computed-tomography/aice_dlr

U = 100 kV
CTDI = 0.6 mGy
DLP = 24.7 mGy·cm
D_{eff} = 0.35 mSv

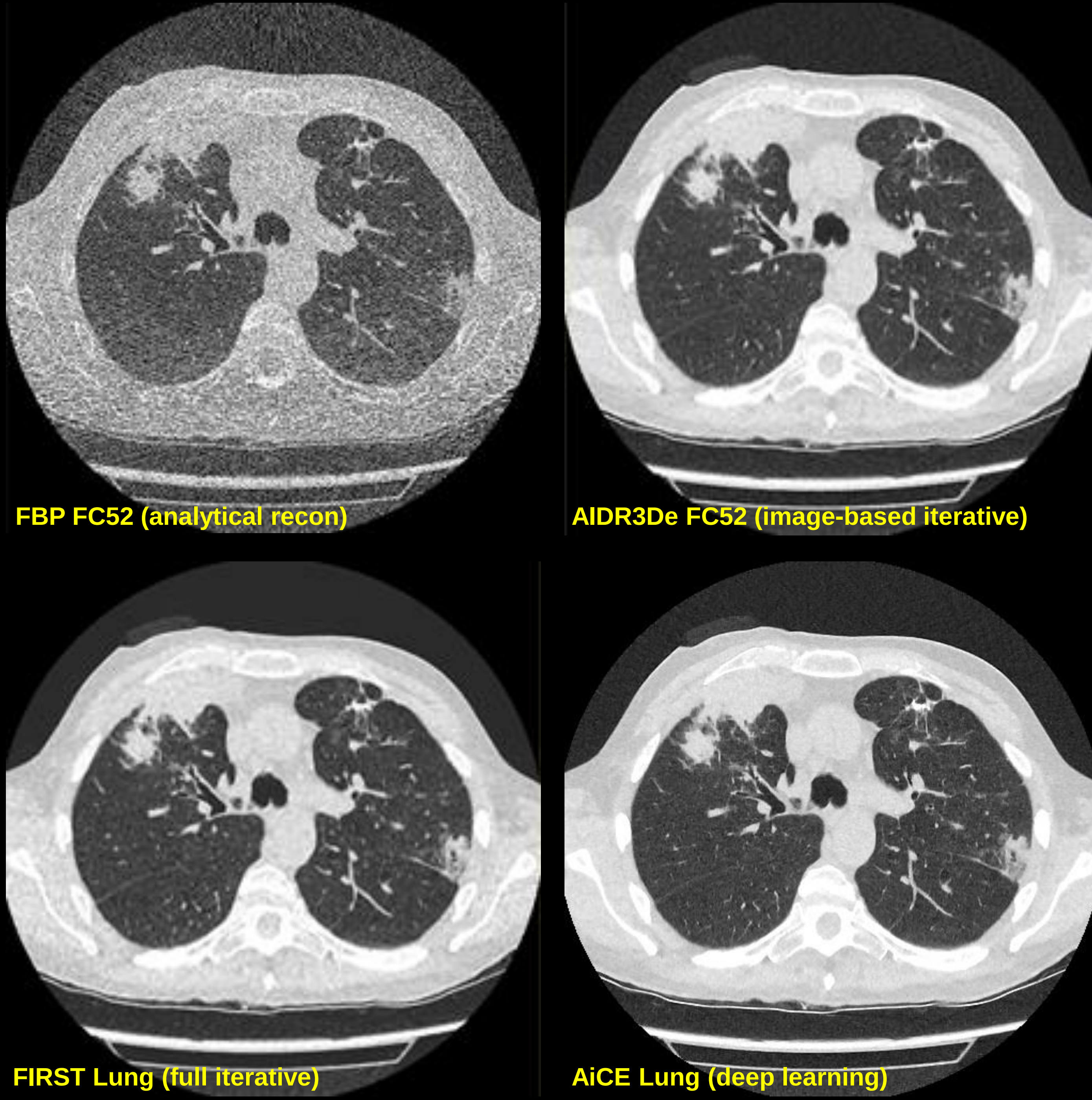

Courtesy of
Radboudumc,
the Netherlands

AIDR 3D

First

AiCE

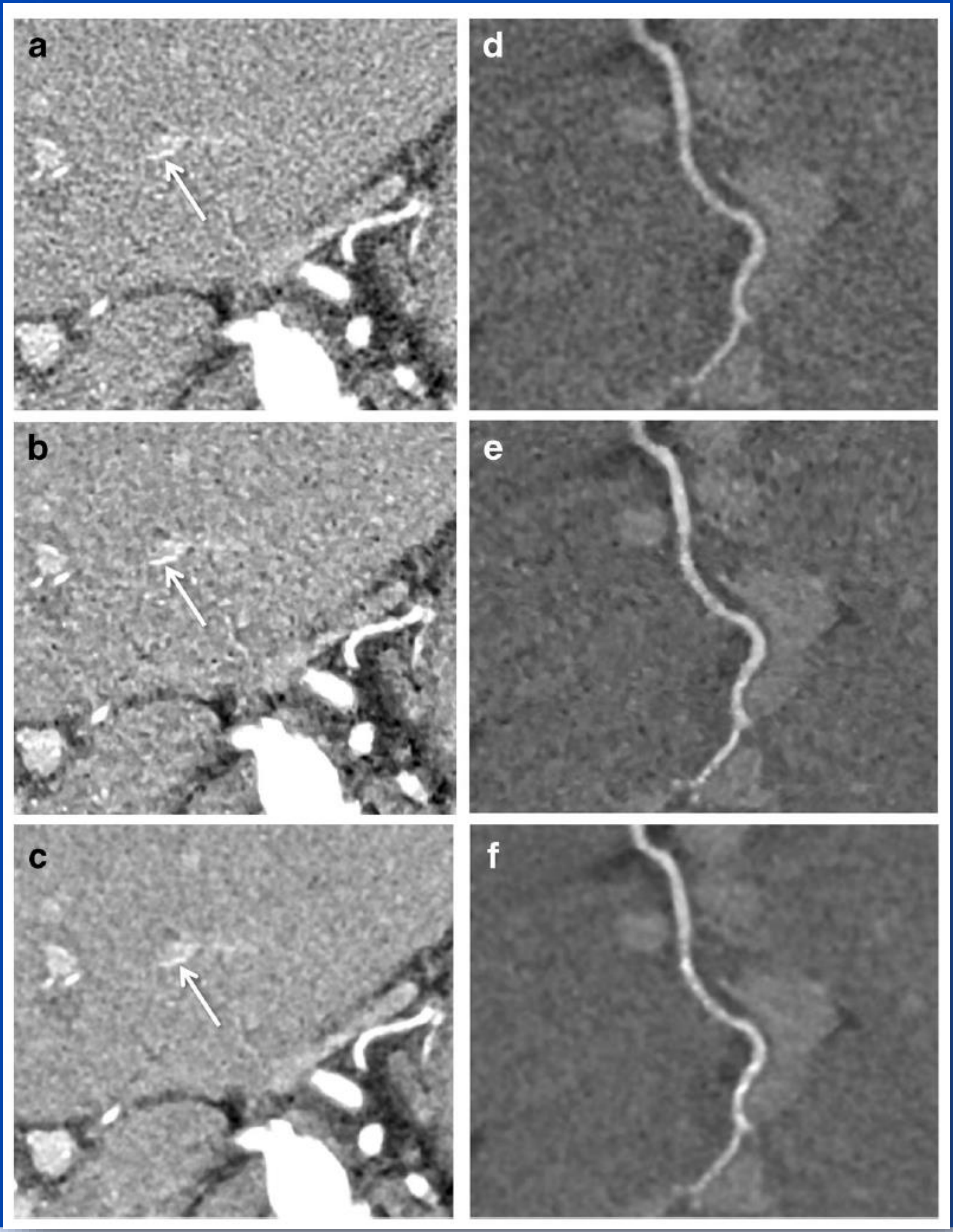

Akagi et al., Deep learning reconstruction improves image quality of abdominal ultra-high-resolution CT, Eur. Radiol. 2019

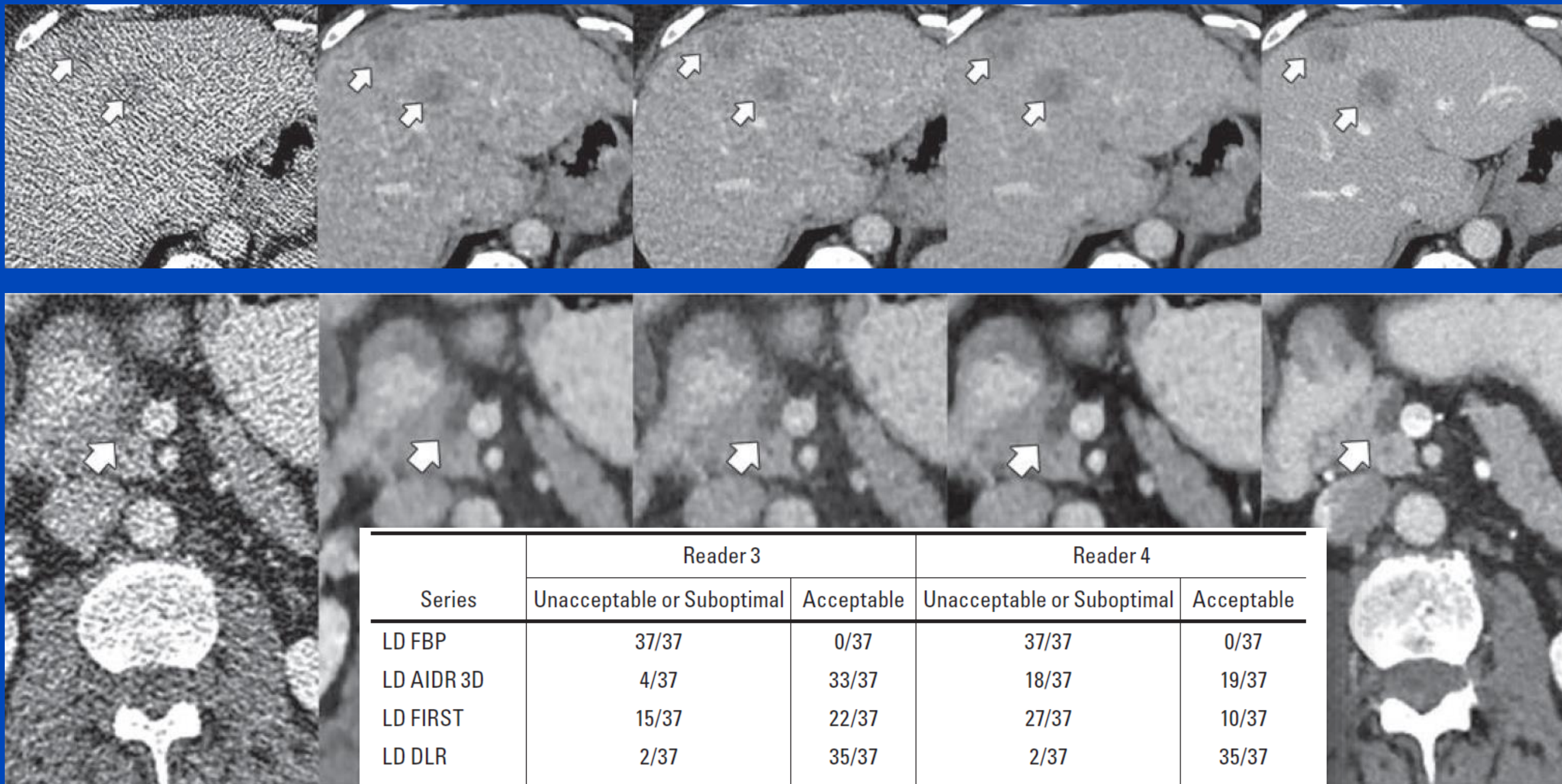

Series	Reader 3		Reader 4	
	Unacceptable or Suboptimal	Acceptable	Unacceptable or Suboptimal	Acceptable
LD FBP	37/37	0/37	37/37	0/37
LD AIDR 3D	4/37	33/37	18/37	19/37
LD FIRST	15/37	22/37	27/37	10/37
LD DLR	2/37	35/37	2/37	35/37
SD AIDR 3D	0/37	37/37	0/37	37/37

Low Dose CT
2 mGy CTDI (top)
3 mGy CTDI (bottom)

Standard Dose CT
19 mGy CTDI (top)
18 mGy CTDI (bottom)

Singh et al., Image Quality and Lesion Detection on Deep Learning Reconstruction and Iterative Reconstruction of Submillisievert Chest and Abdominal CT. AJR 214:566-573, March 2020

Noise Removal Example 7
GE‘s True Fidelity

- Based on a deep CNN
- Trained to restore low-dose CT data to match the properties of Veo, the model-based IR of GE.
- No information can be obtained in how the training is conducted for the product implementation.

2.5D DEEP LEARNING FOR CT IMAGE RECONSTRUCTION USING A MULTI-GPU IMPLEMENTATION

Amirkoushyar Ziabari[⋆], *Dong Hye Ye*[⋆ †], *Somesh Srivastava*[‡], *Ken D. Sauer*[⊕]
Jean-Baptiste Thibault[‡], *Charles A. Bouman*[⋆]

[⋆] Electrical and Computer Engineering at Purdue University
[†] Electrical and Computer Engineering at Marquett University
[‡] GE Healthcare
[⊕] Electrical Engineering at University of Notre Dame

ABSTRACT

While Model Based Iterative Reconstruction (MBIR) of CT scans has been shown to have better image quality than Filtered Back Projection (FBP), its use has been limited by its high computational cost. More recently, deep convolutional neural networks (CNN) have shown great promise in both denoising and reconstruction applications. In this research, we propose a fast reconstruction algorithm, which we call Deep

streaking artifacts caused by sparse projection views in CT images [8]. More recently, Ye, et al. [9] developed method for incorporating CNN denoisers into MBIR reconstruction as advanced prior models using the Plug-and-Play framework [10, 11].

In this paper, we propose a fast reconstruction algorithm, which we call Deep Learning MBIR (DL-MBIR), for approximately achieving the improved quality of MBIR using a deep residual neural network. The DL-MBIR method is trained to

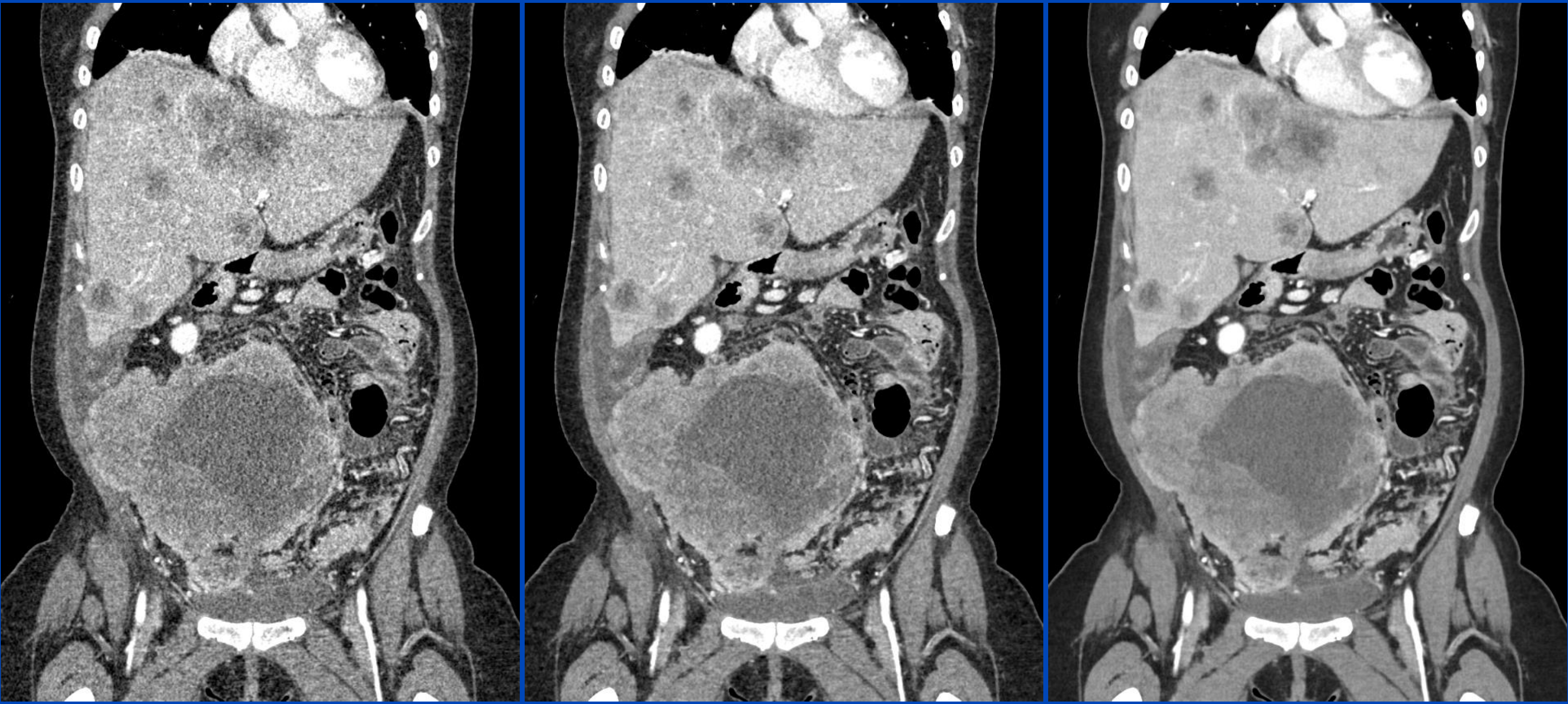

FBP

ASIR V 50%

True Fidelity

Courtesy of GE Healthcare

Part 3:

Fast Physics

Deep Scatter Estimation

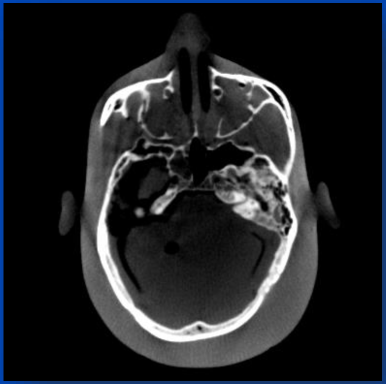

???

In real time?

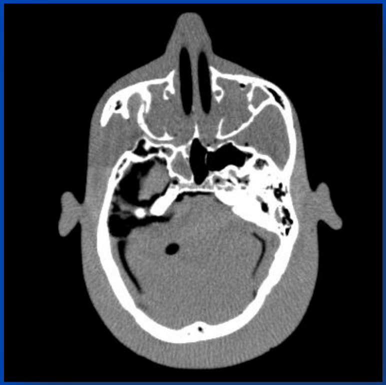

Monte Carlo Scatter Estimation

- Simulation of photon trajectories according to physical interaction probabilities.
- Simulating a large numb… …ries well approximat…

1 to 10 hours
per tomographic data set

mplete scatter distribution

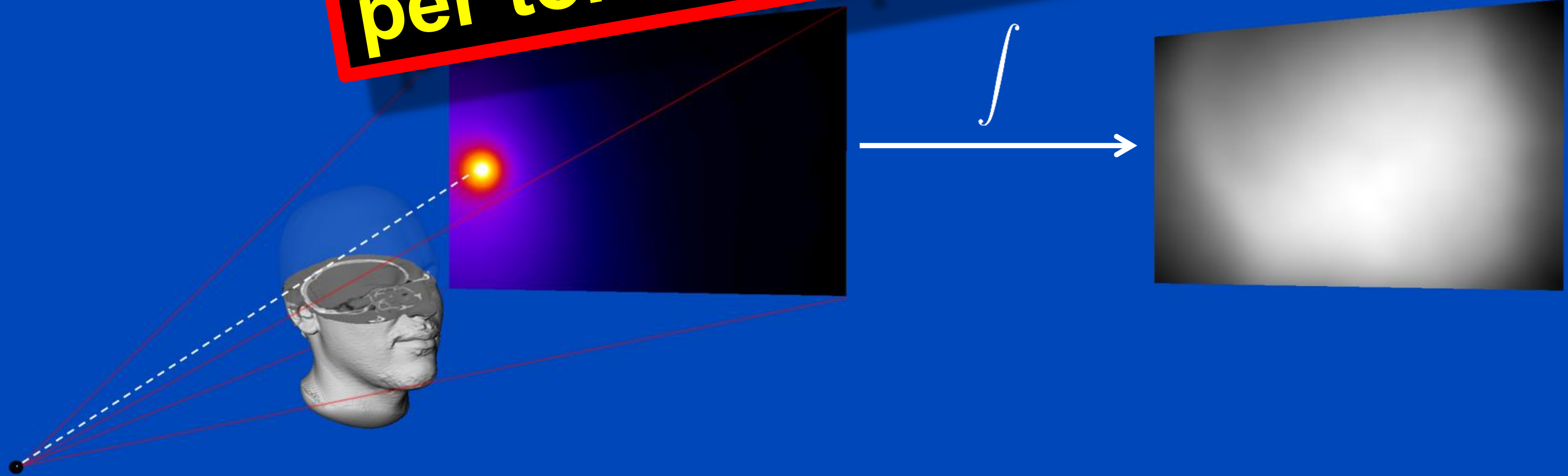

Deep Scatter Estimation

Network architecture & scatter estimation framework

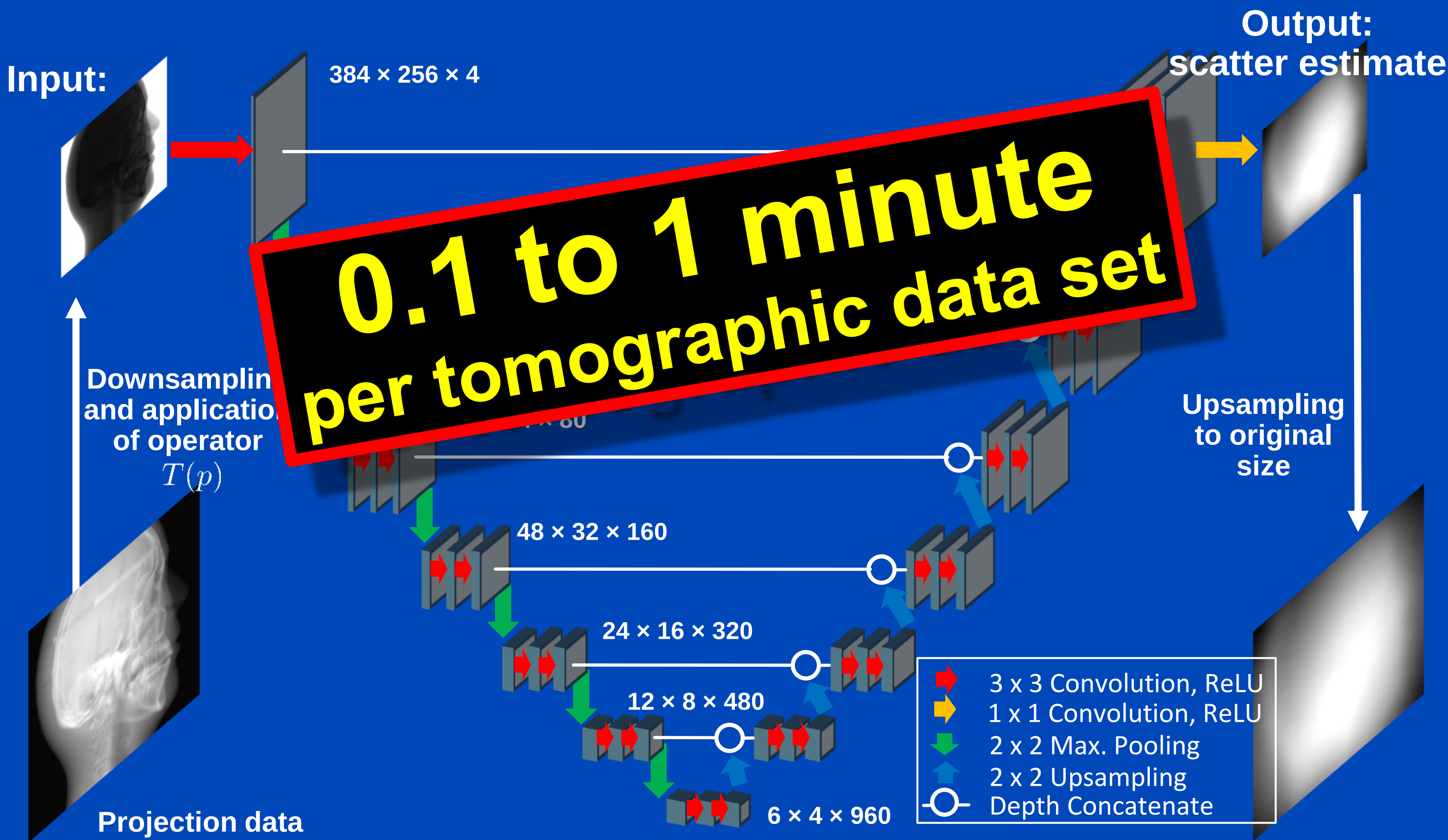

PEP

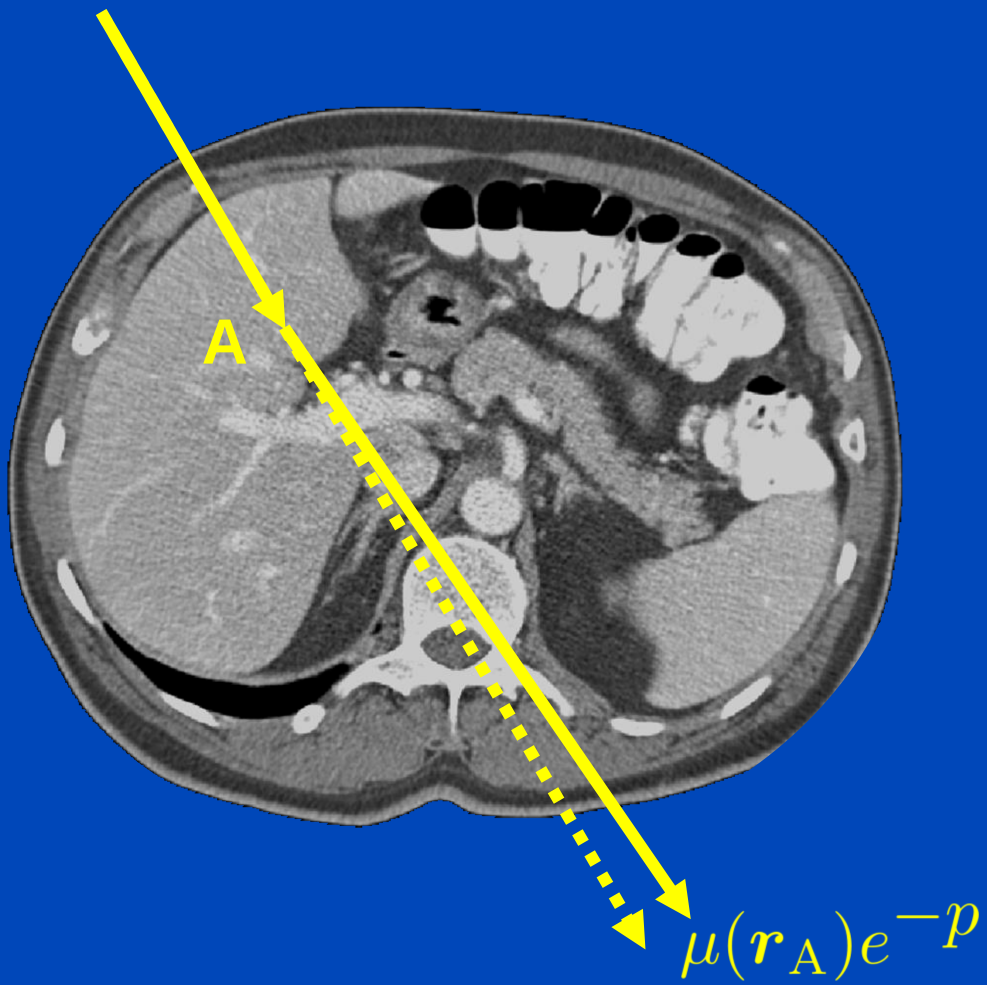

PEP

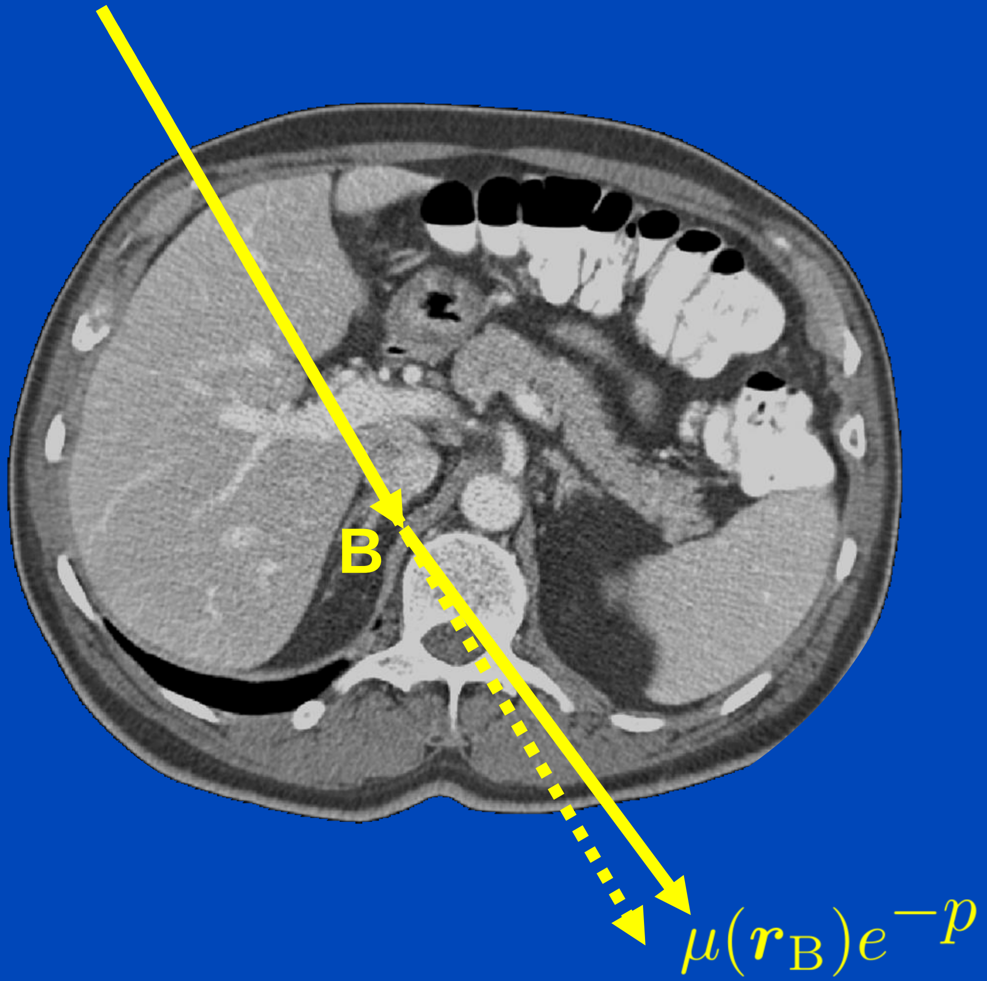

PEP

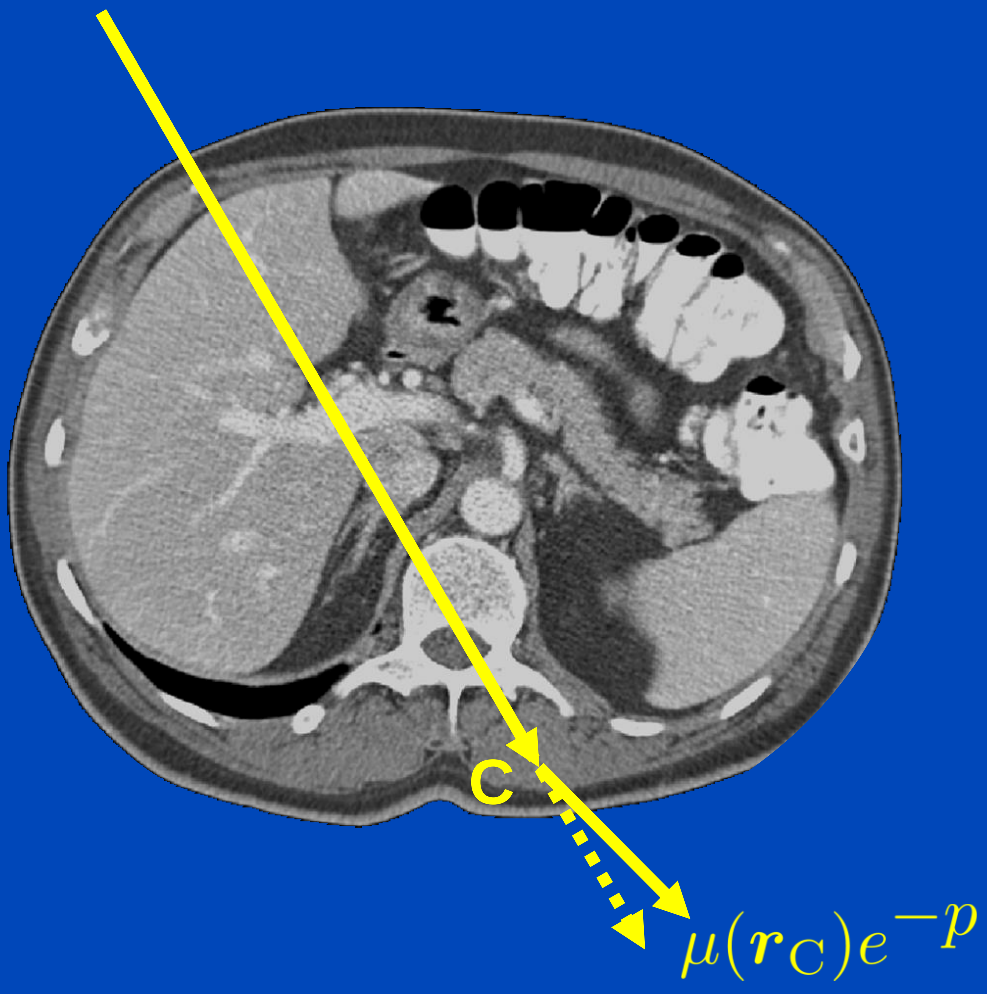

PEP

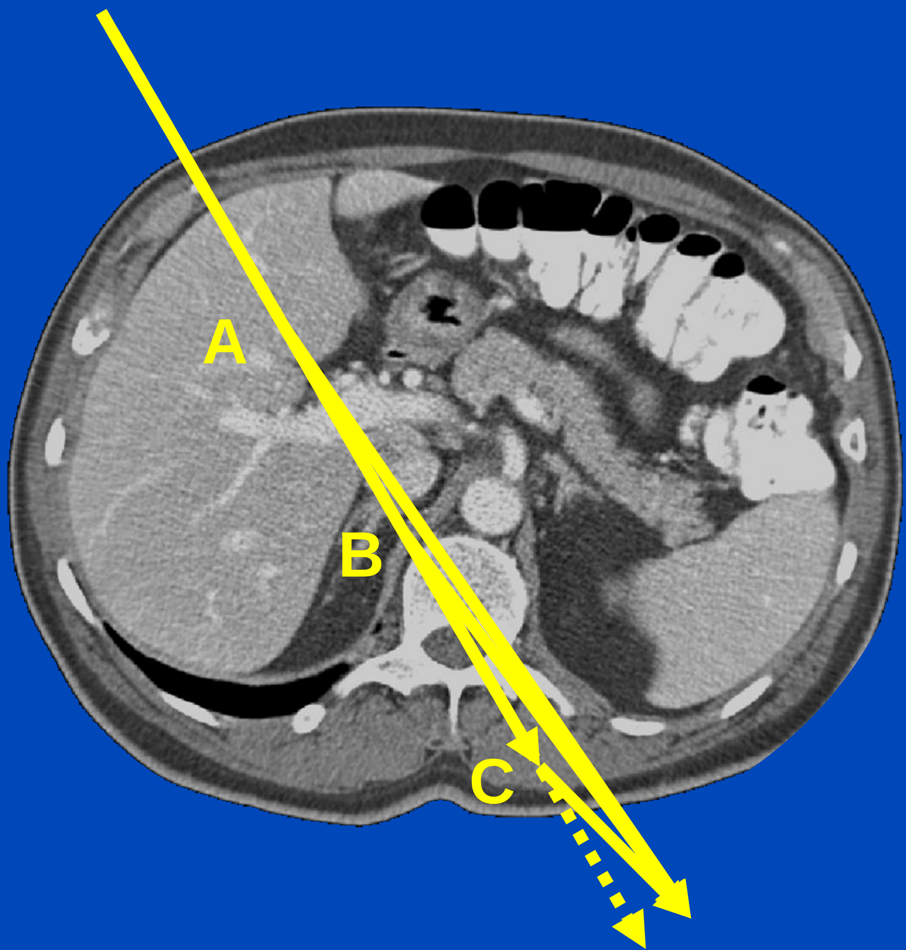

$$\big(\mu(\boldsymbol{r}_{\mathrm{A}})+\mu(\boldsymbol{r}_{\mathrm{B}})+\mu(\boldsymbol{r}_{\mathrm{C}})\big)e^{-p} = p\,e^{-p}$$

Results on Simulated Projection Data

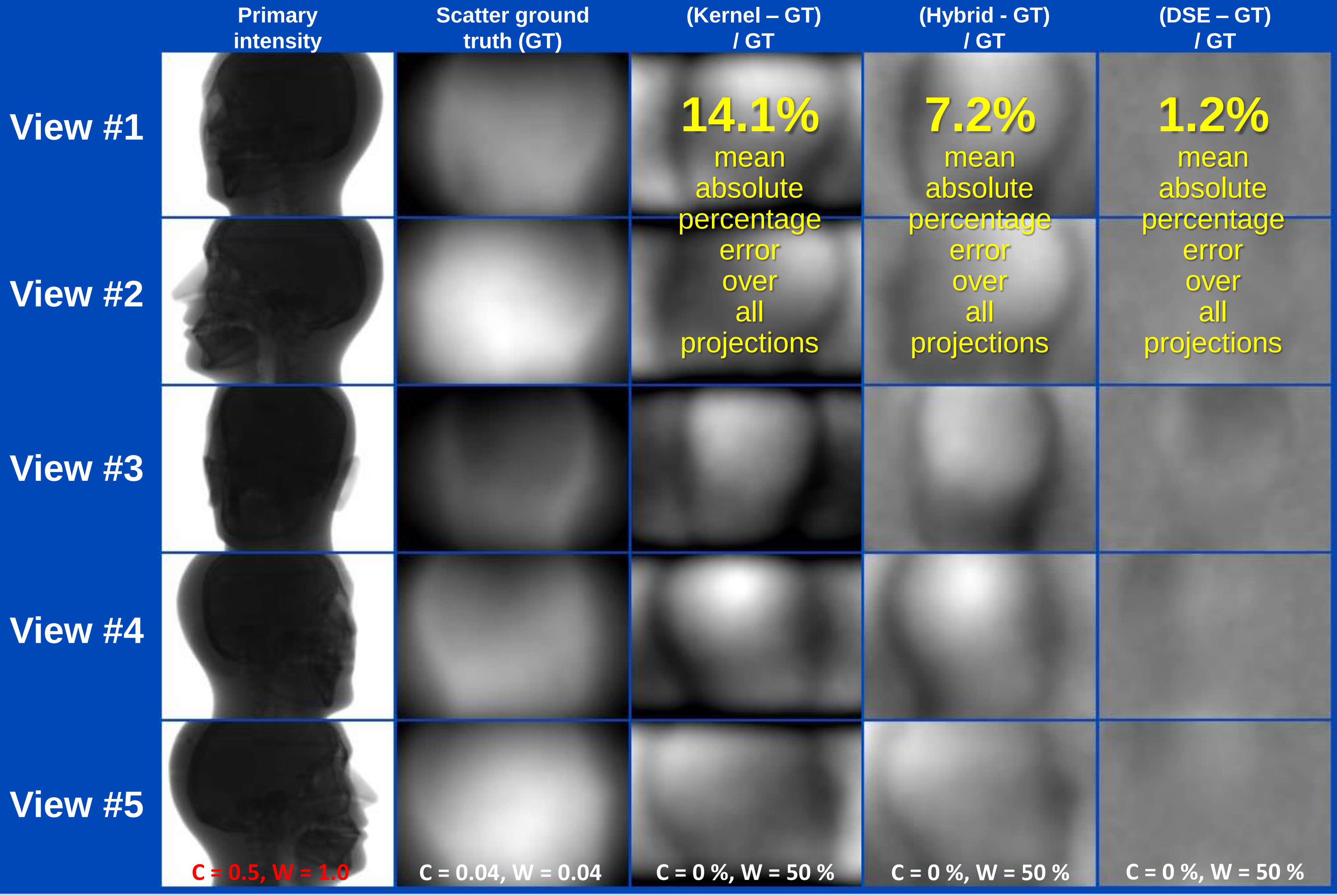

DSE trained to estimate scatter from **primary plus scatter**: High accuracy

dkfz.

Results on Simulated Projection Data

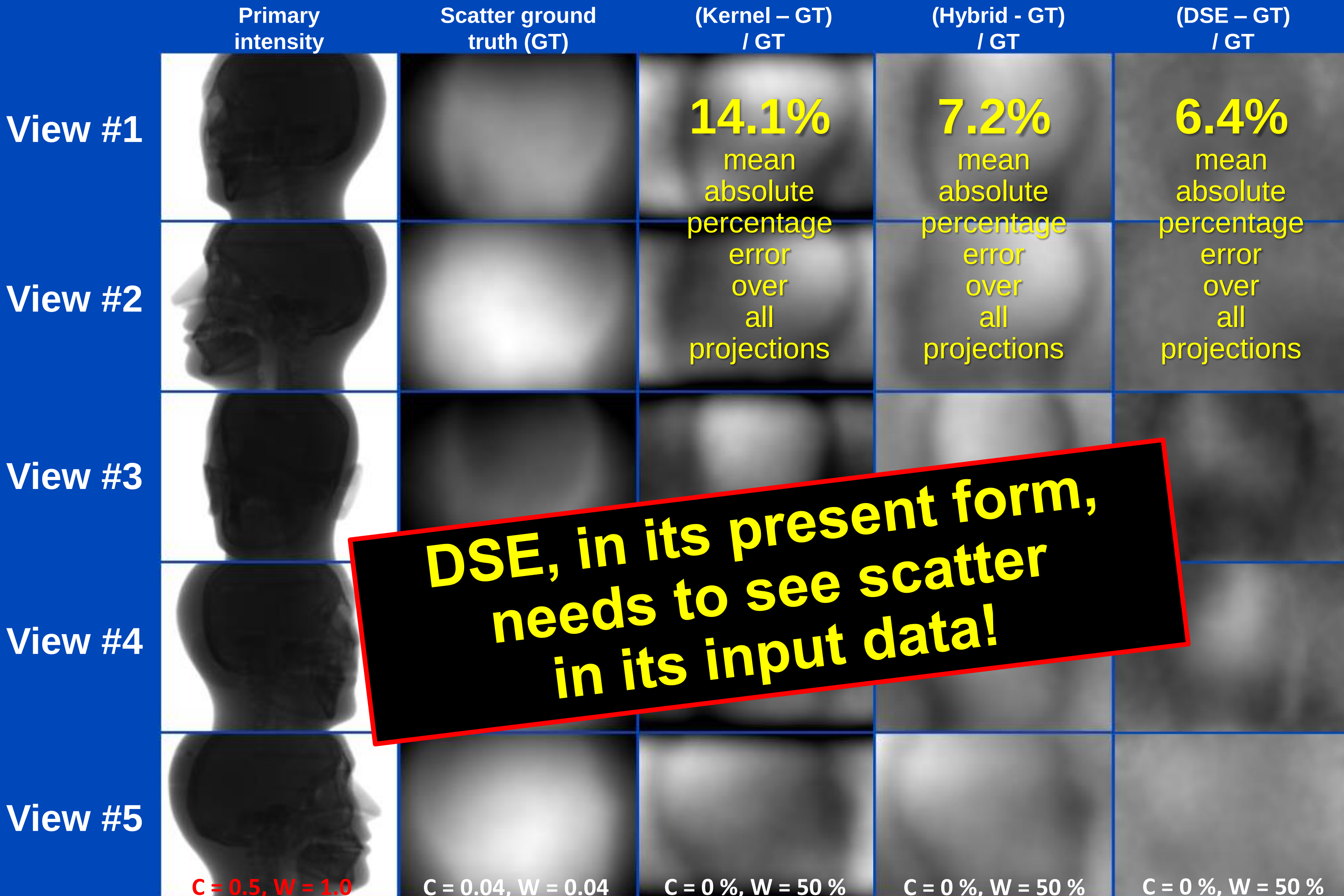

DSE trained to estimate scatter from **primary only**: Low accuracy

dkfz.

Results on Simulated Projection Data

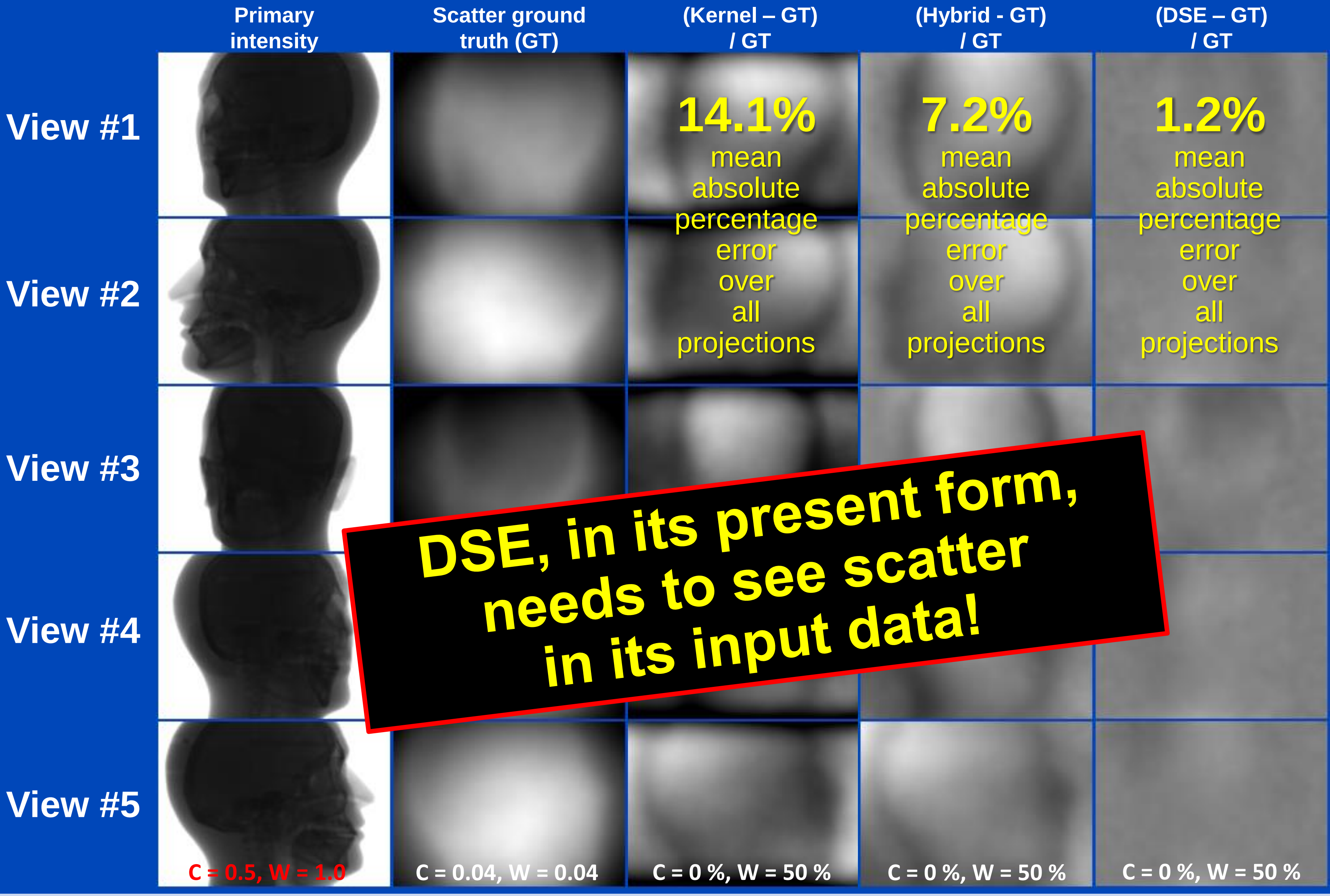

DSE trained to estimate scatter from **primary plus scatter**: High accuracy

Reconstructions of Simulated Data

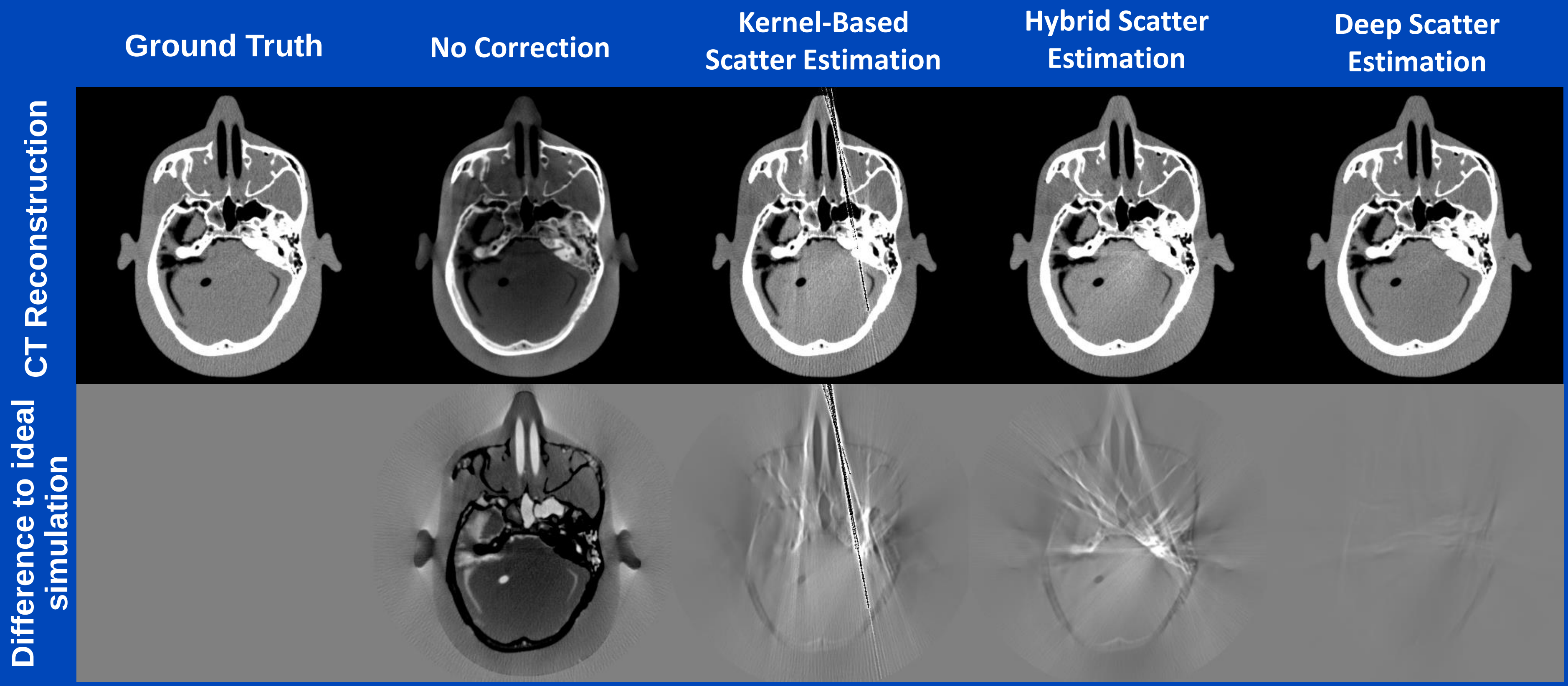

C = 0 HU, W = 1000 HU

J. Maier, M. Kachelrieß et al. Deep scatter estimation (DSE). SPIE 2017 and Journal of Nondestructive Evaluation 37:57, July 2018.
J. Maier, M. Kachelrieß et al. Robustness of DSE. Med. Phys. 46(1):238-249, January 2019.

Testing of the DSE Network for Measured Data (120 kV)

DKFZ table-top CT

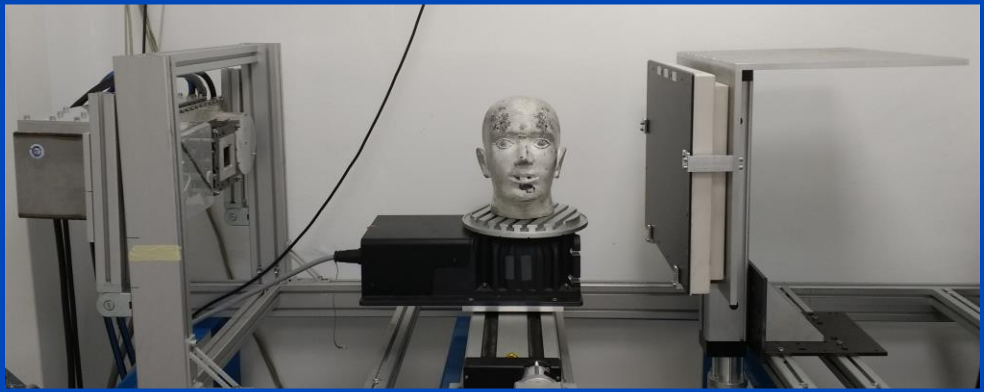

- Measurement of a head phantom at our in-house table-top CT.
- Slit scan measurement serves as ground truth.

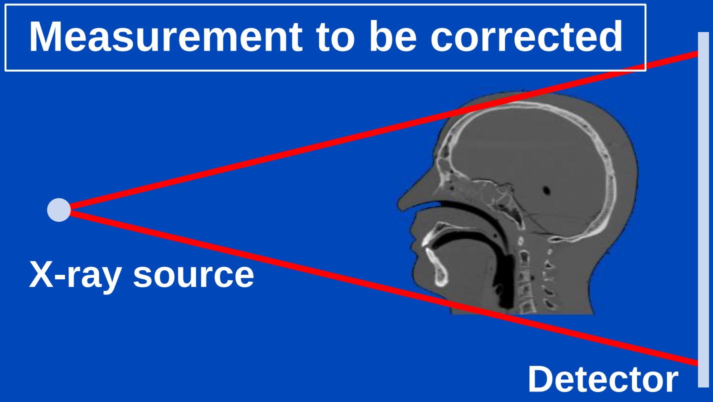

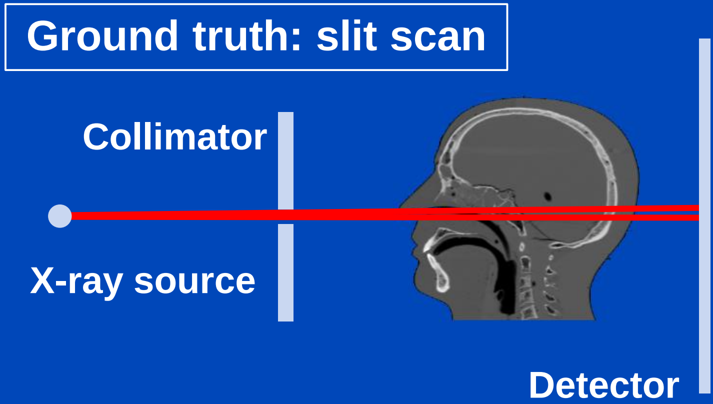

J. Maier, M. Kachelrieß et al. Deep scatter estimation (DSE). SPIE 2017 and Journal of Nondestructive Evaluation 37:57, July 2018.
J. Maier, M. Kachelrieß et al. Robustness of DSE. Med. Phys. 46(1):238-249, January 2019.

Reconstructions of Measured Data

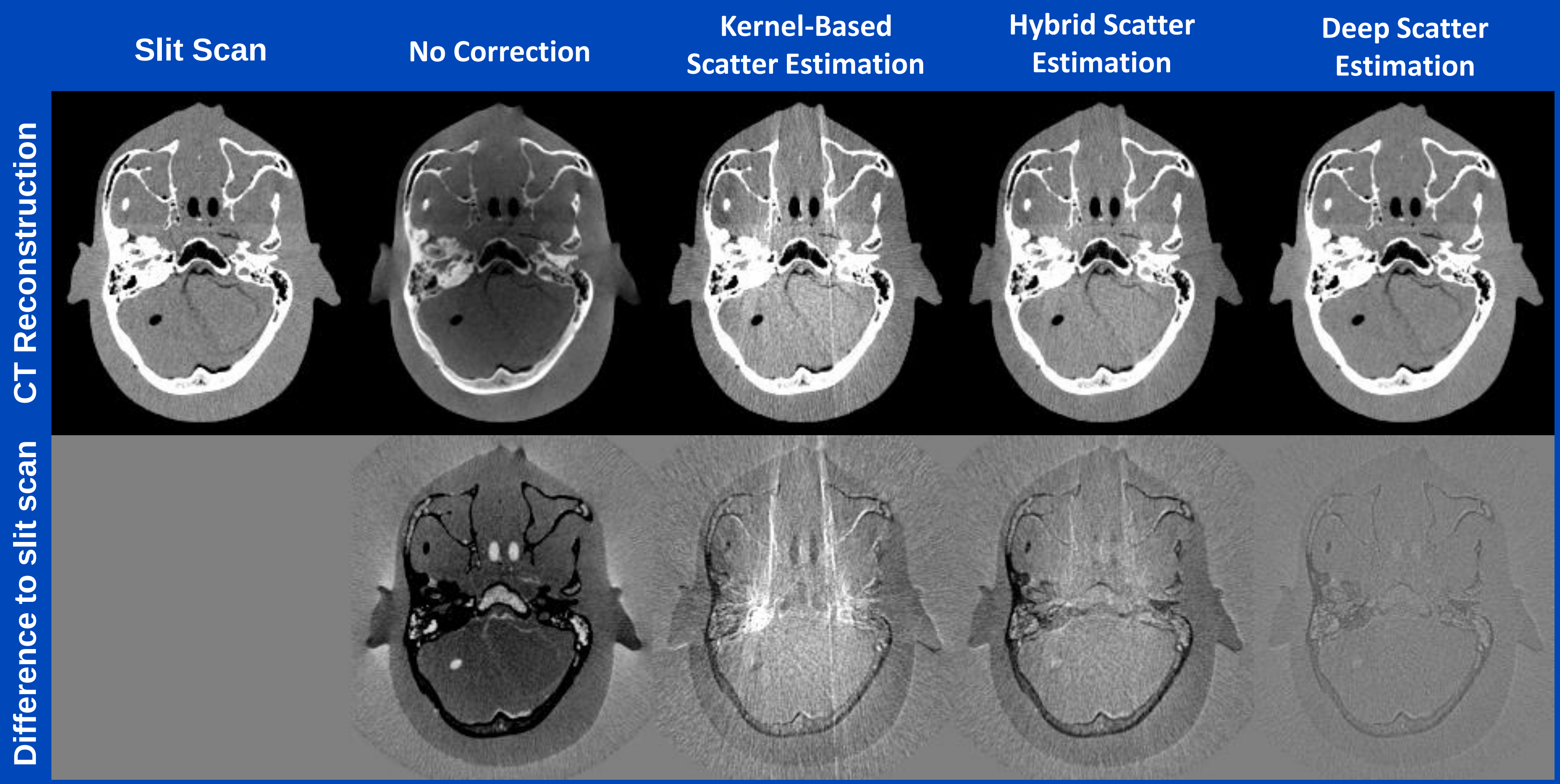

C = 0 HU, *W* = 1000 HU

J. Maier, M. Kachelrieß et al. Deep scatter estimation (DSE). SPIE 2017 and Journal of Nondestructive Evaluation 37:57, July 2018.
J. Maier, M. Kachelrieß et al. Robustness of DSE. Med. Phys. 46(1):238-249, January 2019.

A simple detruncation was applied to the rawdata before reconstruction. Images were clipped to the FOM before display. C = -200 HU, W = 1000 HU.

Truncated DSE[1,2]

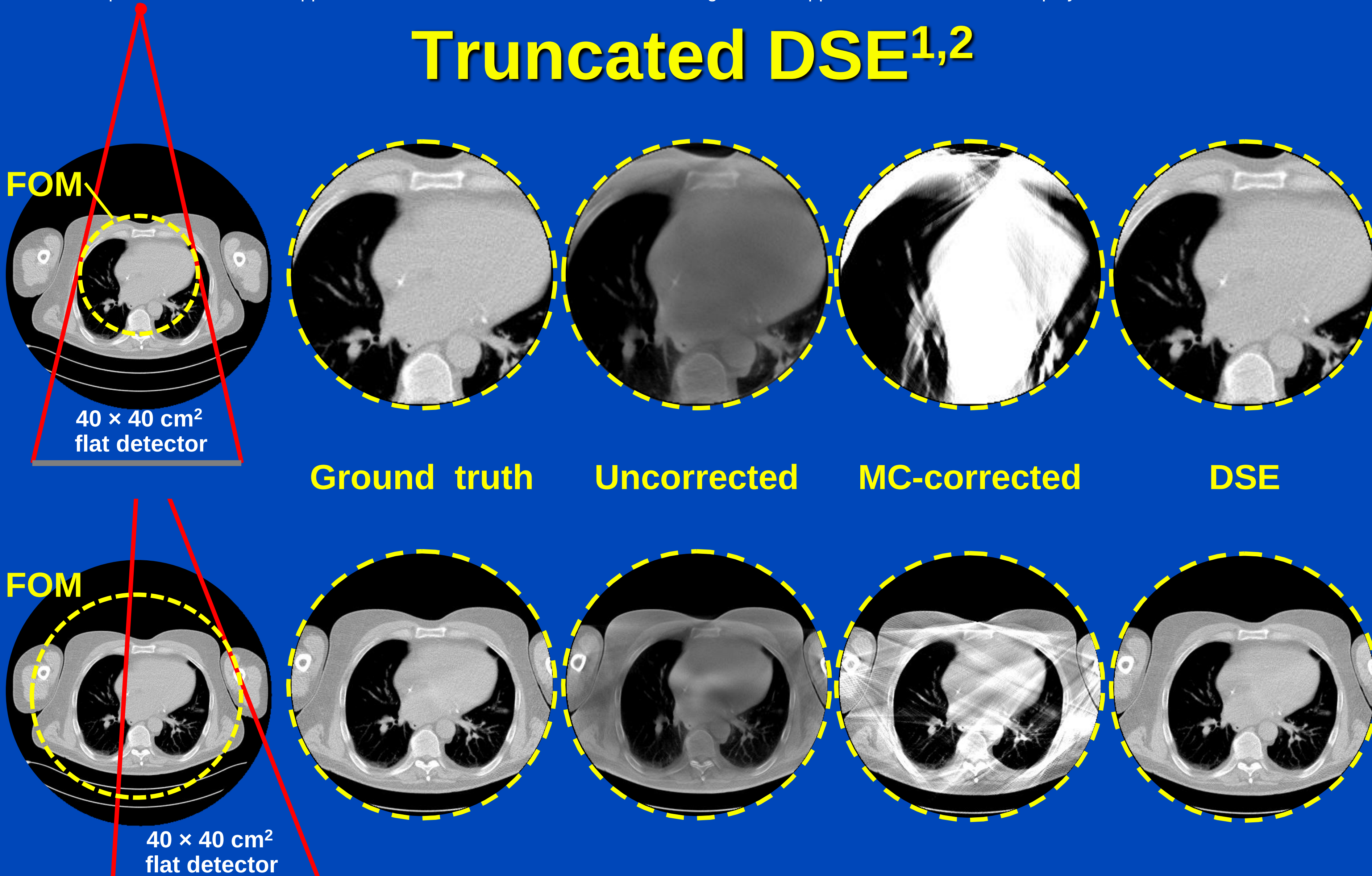

To learn why MC fails at truncated data and what significant efforts are necessary to cope with that situation see [Kachelrieß et al. Effect of detruncation on the accuracy of MC-based scatter estimation in truncated CBCT. Med. Phys. 45(8):3574-3590, August 2018].

[1] J. Maier, M. Kachelrieß et al. Deep scatter estimation (DSE) for truncated cone-beam CT (CBCT). RSNA 2018.
[2] J. Maier, M. Kachelrieß et al. Robustness of DSE. Med. Phys. 46(1):238-249, January 2019.

dkfz.

Scatter in Dual Source CT (DSCT)

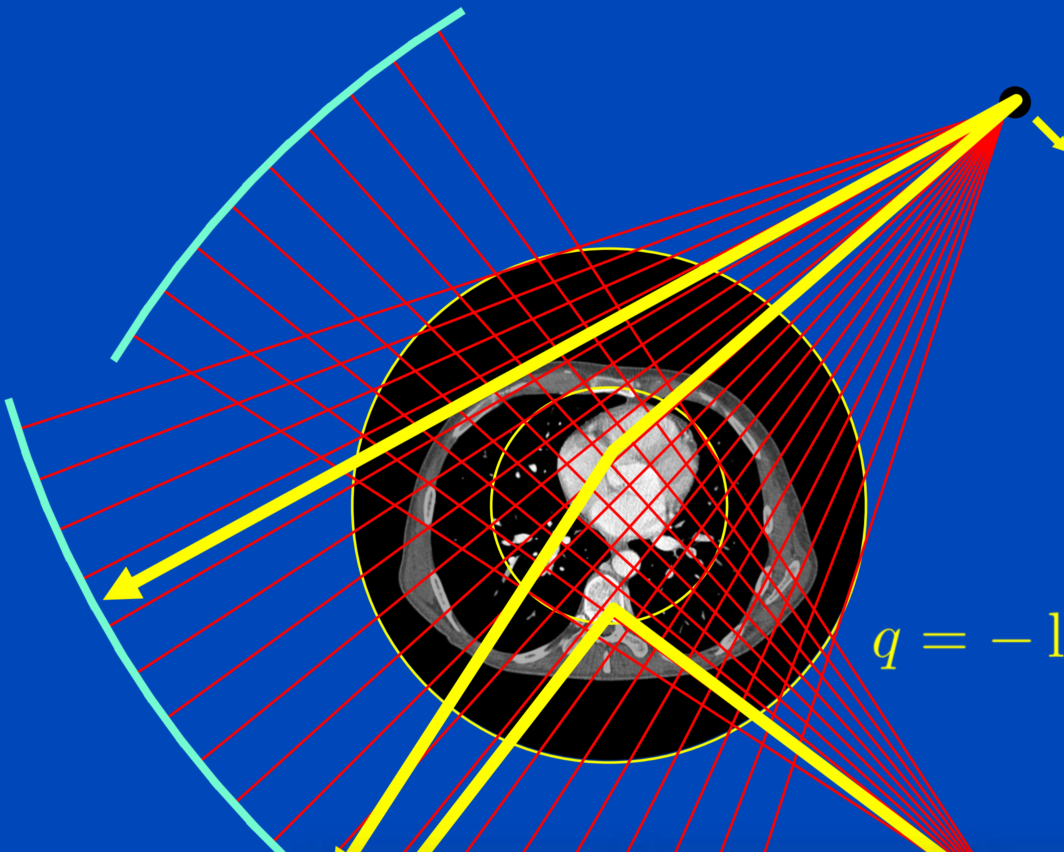

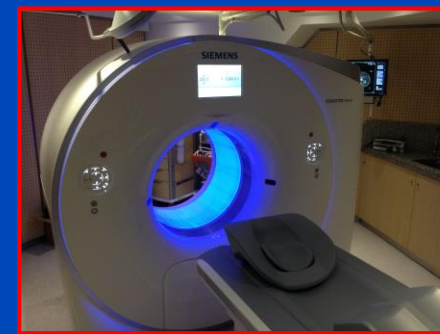

Siemens SOMATOM Force
dual source cone-beam spiral CT

$$q = -\ln \frac{I_{\text{primary}} + S_{\text{forward}} + \rho\, S_{\text{cross}}}{I_0}$$

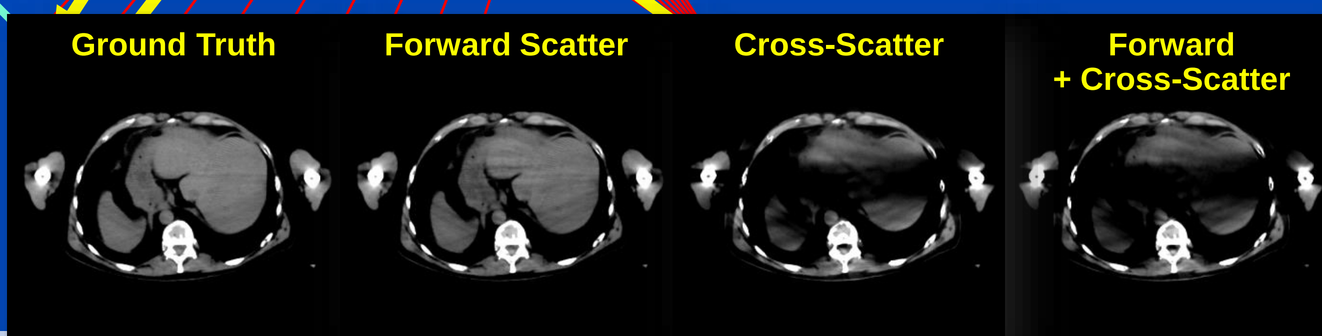

C = 40 HU, *W* = 300 HU, with 2D anti-scatter grid

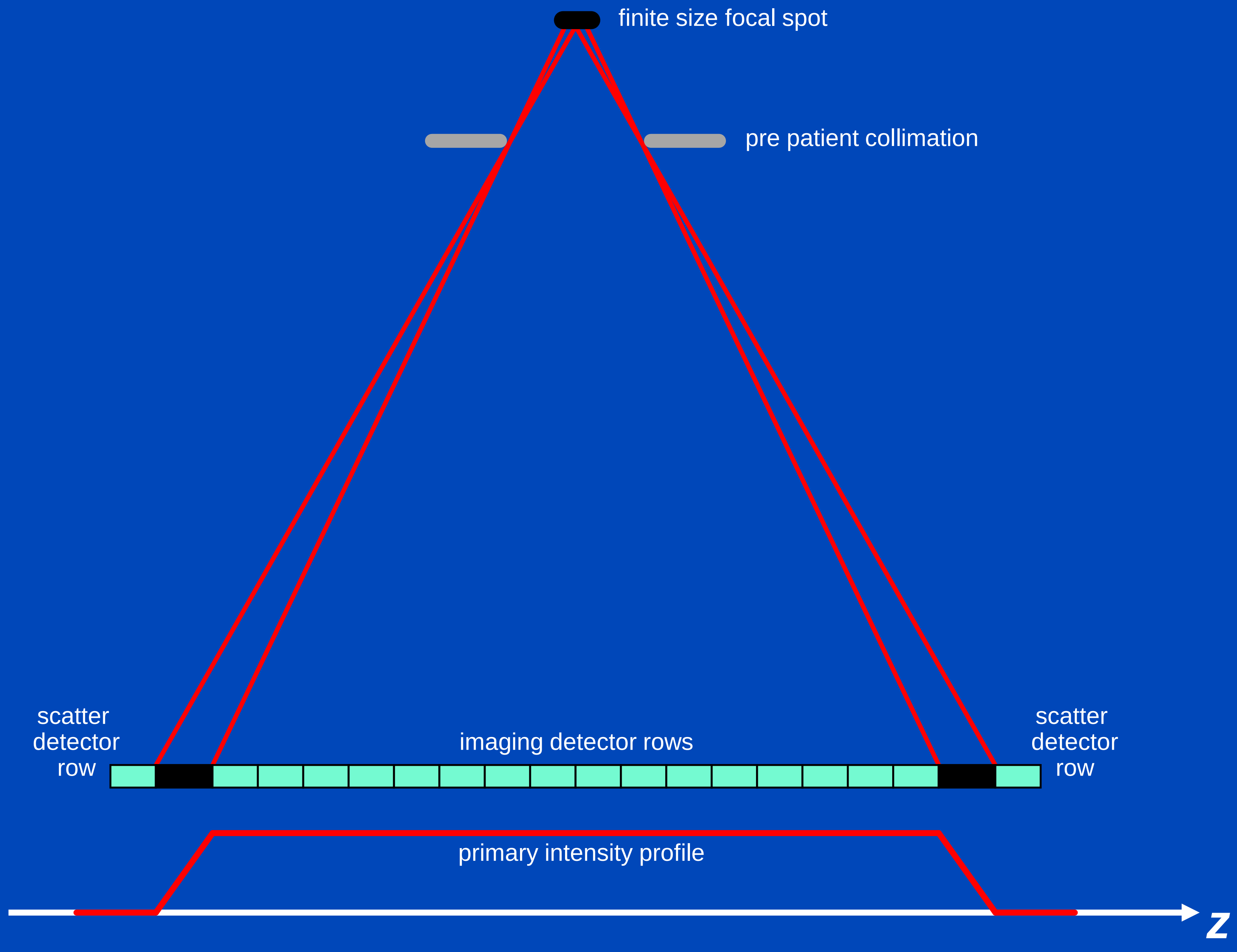
finite size focal spot
pre patient collimation
scatter detector row
imaging detector rows
scatter detector row
primary intensity profile
z

Cross-DSE

Ground Truth | **Uncorrected** | **xDSE (2D, xSSE)** | **Measurement-based**

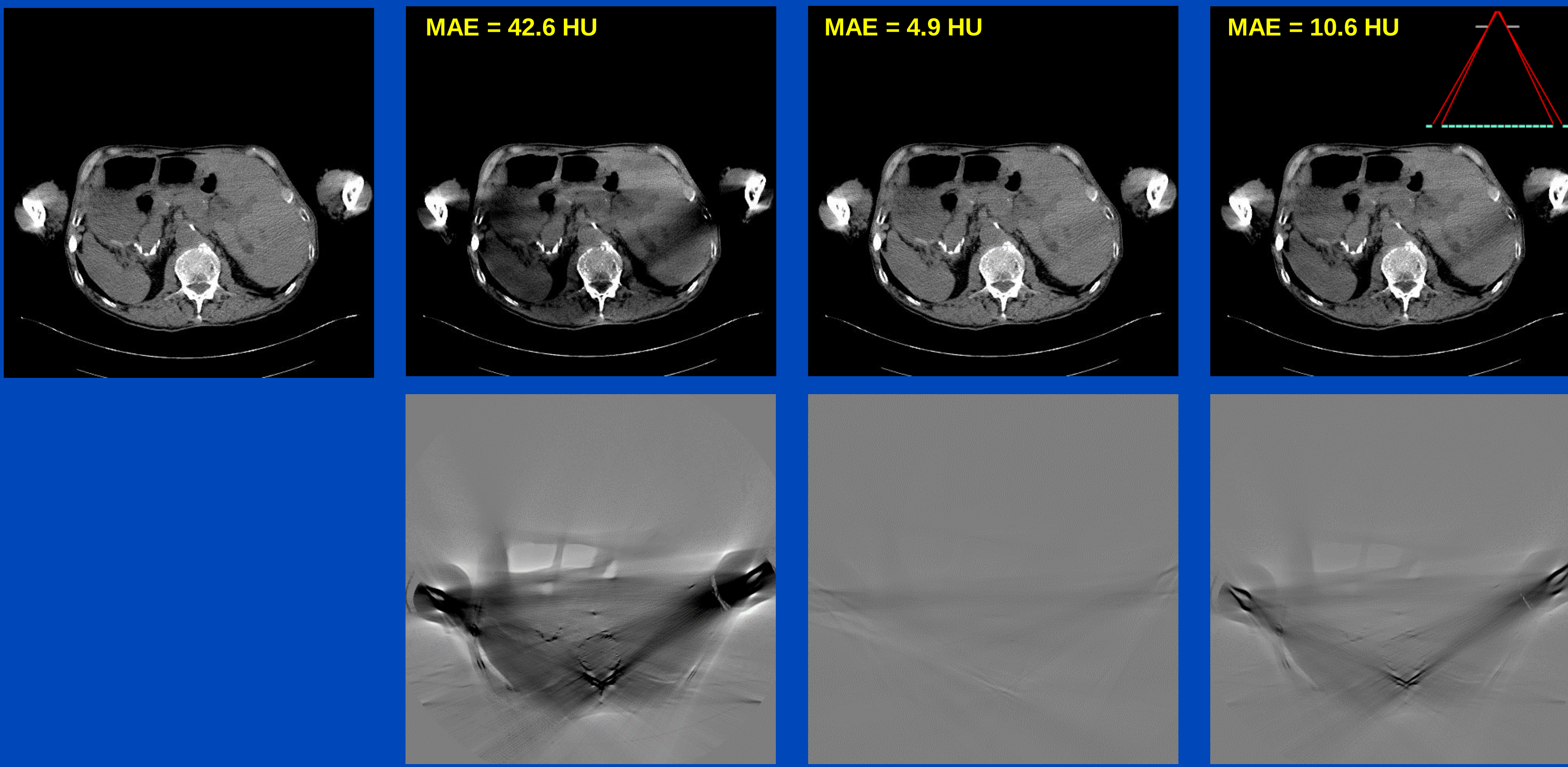

xDSE (2D, xSSE) maps
primary + forward scatter + cross-scatter + cross-scatter approximation → cross-scatter

Images C = 40 HU, W = 300 HU, difference images C = 0 HU, W = 300 HU

J. Erath, M. Kachelrieß et al. Deep learning-based cross-scatter correction for clinical CT. Conference Program of the 6th International Conference on Image Formation in X-Ray Computed Tomography:412-415, August 2020.

Conclusions on DSE

- DSE needs about 3 ms per CT and 10 ms per CBCT projection (as of 2020).
- DSE is a fast and accurate alternative to MC simulations.
- DSE outperforms kernel-based approaches in terms of accuracy and speed.
- Facts:
  - DSE can estimate scatter from a single (!) x-ray image.
  - DSE can accurately estimate scatter from a primary+scatter image.
  - DSE generalizes to all anatomical regions.
  - DSE works for geometries and beam qualities differing from training.
  - DSE may outperform MC even though DSE is trained with MC.
- DSE is not restricted to reproducing MC scatter estimates.
- DSE can rather be trained with any other scatter estimate, including those based on measurements.

Deep Dose Estimation

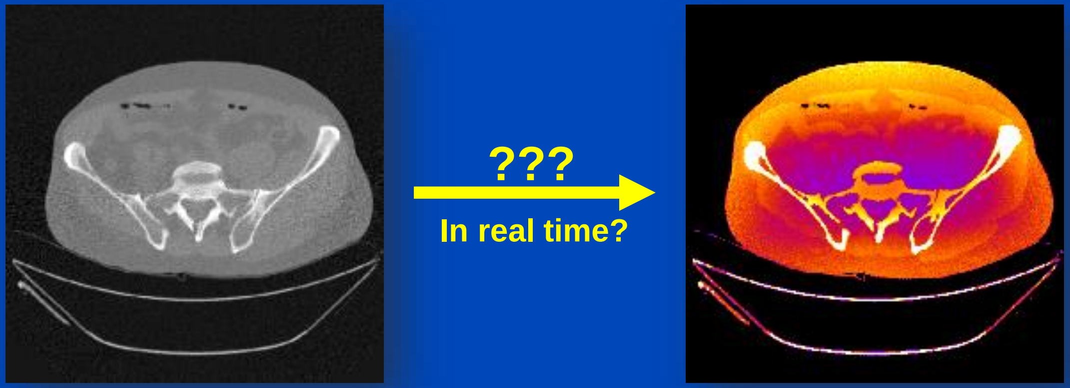

Deep Dose Estimation (DDE)

- Combine fast and accurate CT dose estimation using a deep convolutional neural network.
- Train the network to reproduce MC dose estimates given the CT image and a first-order dose estimate.

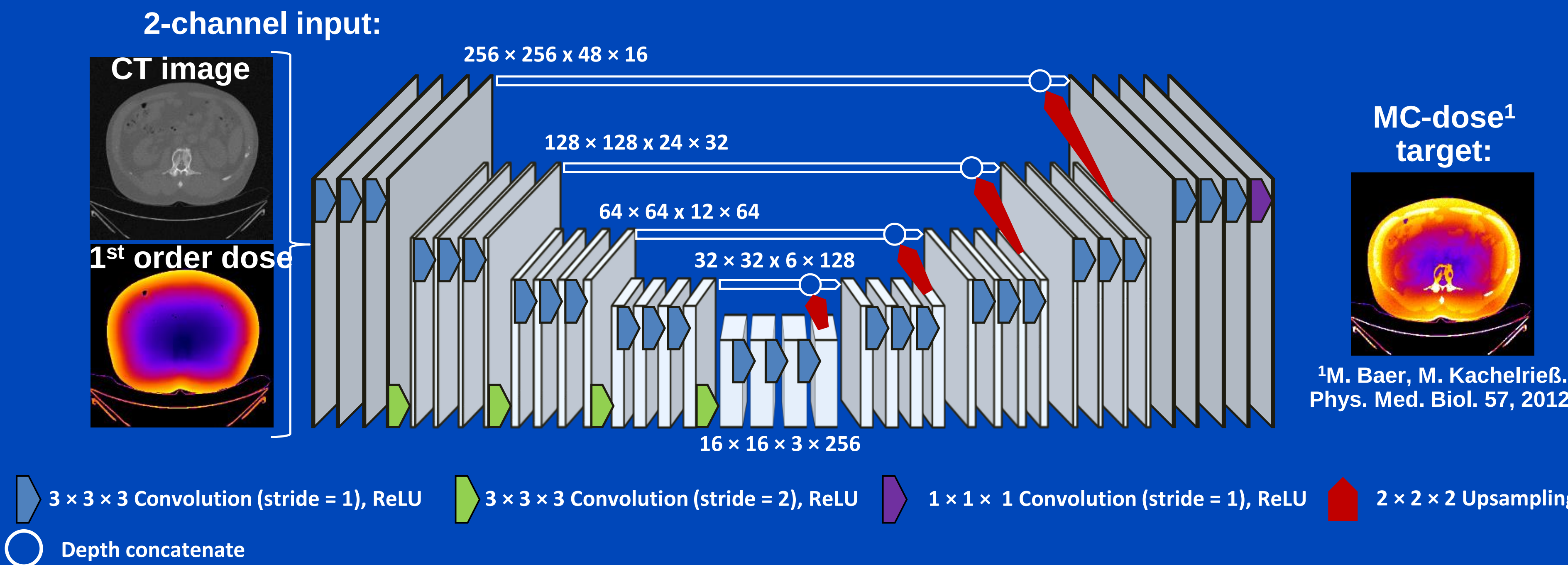

Results

Thorax, tube A, 120 kV, with bowtie

CT image

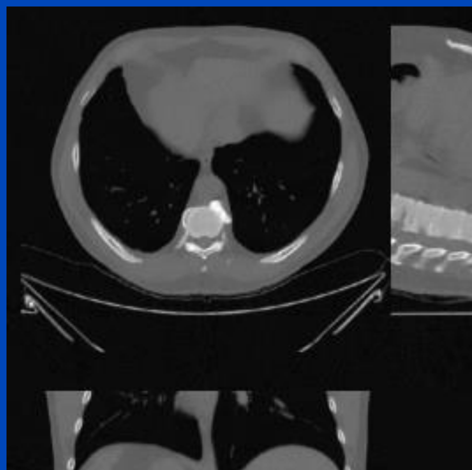

First order dose

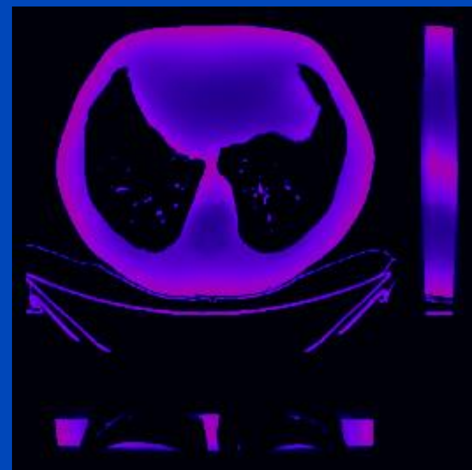

	MC	DDE
48 slices	1 h	0.25 s
whole body	20 h	5 s

MC uses 16 CPU kernels
DDE uses one Nvidia Quadro P600 GPU

DDE training took 74 h for 300 epochs, 1440 samples, 48 slices per sample

MC ground truth

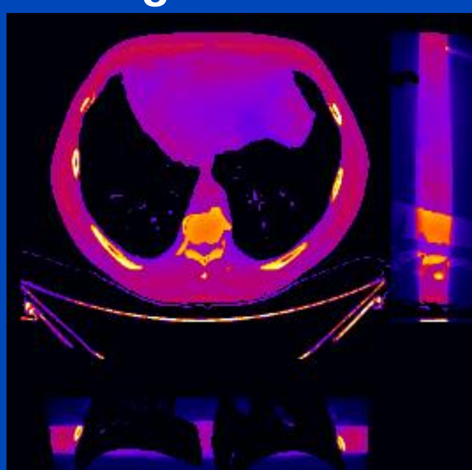

DDE

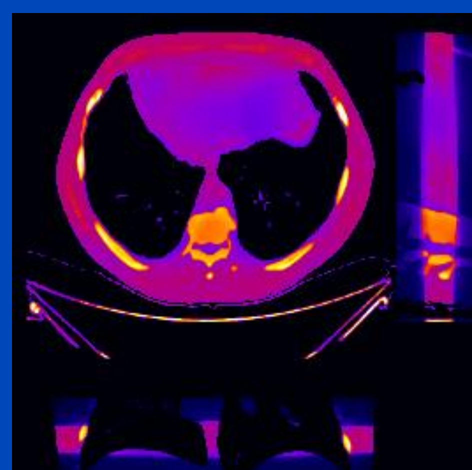

Relative error

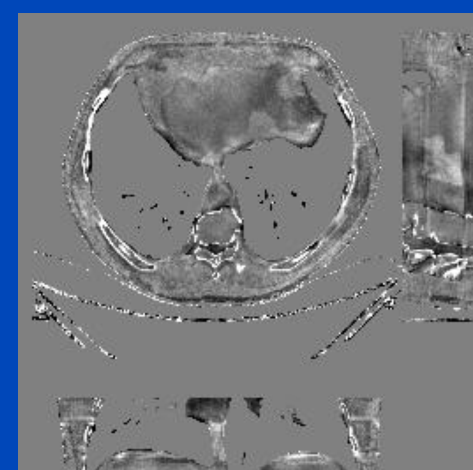

C = 0%
W = 40%

J. Maier, E. Eulig, S. Sawall, and M. Kachelrieß. Real-time patient-specific CT dose estimation using a deep convolutional neural network, Proc. IEEE MIC 2018 and ECR Book of Abstracts 2019. *Best Paper within Machine Learning at ECR 2019!*

Results

Thorax, tube A, 120 kV, no bowtie

CT image

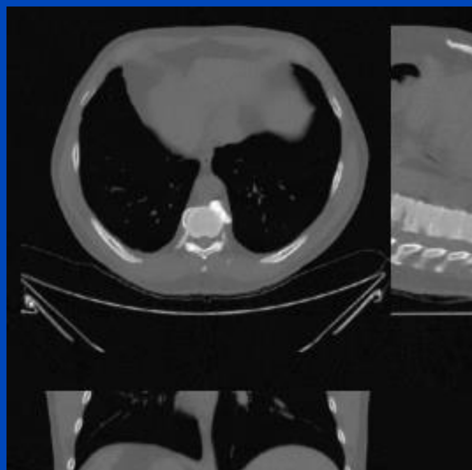

First order dose

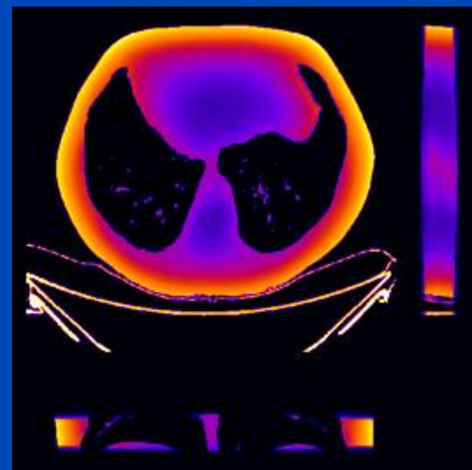

	MC	DDE
48 slices	1 h	0.25 s
whole body	20 h	5 s

MC uses 16 CPU kernels
DDE uses one Nvidia Quadro P600 GPU

DDE training took 74 h for 300 epochs, 1440 samples, 48 slices per sample

MC ground truth

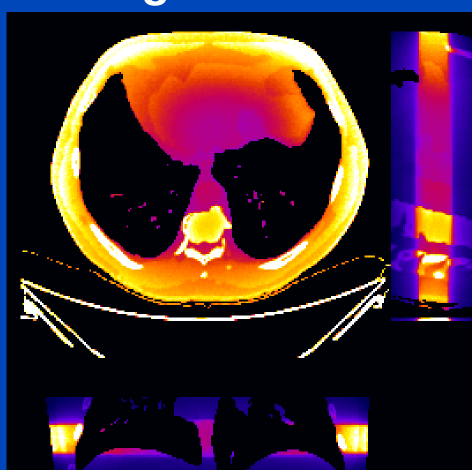

DDE

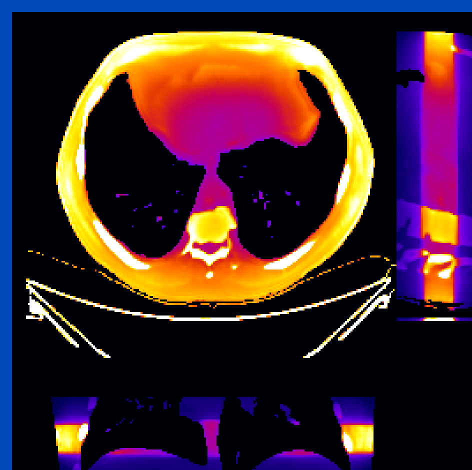

Relative error

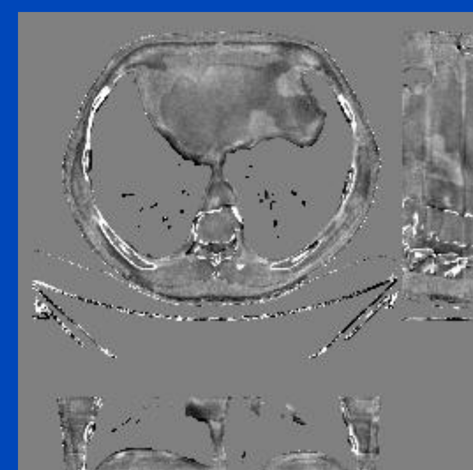

C = 0%
W = 40%

J. Maier, E. Eulig, S. Sawall, and M. Kachelrieß. Real-time patient-specific CT dose estimation using a deep convolutional neural network, Proc. IEEE MIC 2018 and ECR Book of Abstracts 2019. *Best Paper within Machine Learning at ECR 2019!*

Results

Thorax, tube B, 120 kV, no bowtie

CT image

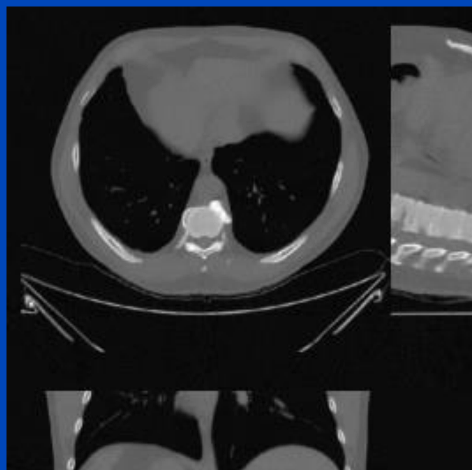

First order dose

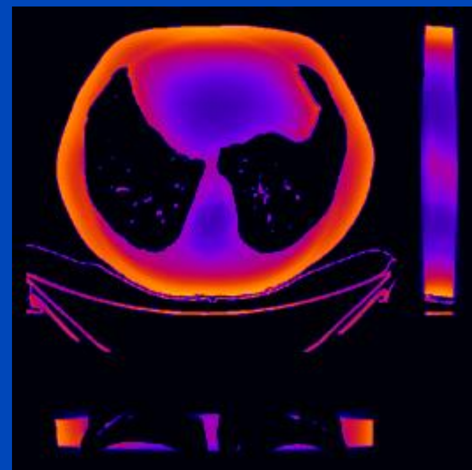

	MC	DDE
48 slices	1 h	0.25 s
whole body	20 h	5 s

MC uses 16 CPU kernels
DDE uses one Nvidia Quadro P600 GPU

DDE training took 74 h for 300 epochs, 1440 samples, 48 slices per sample

MC ground truth

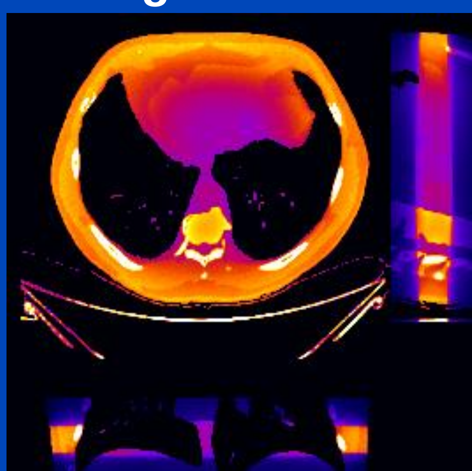

DDE

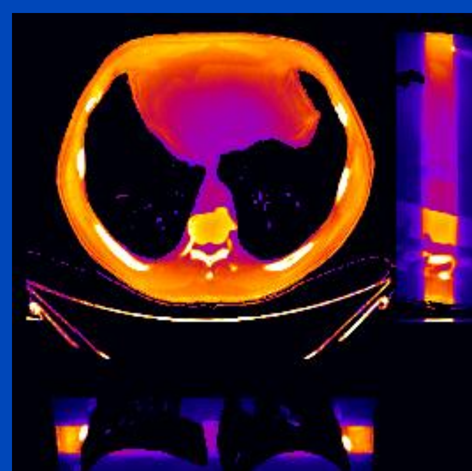

Relative error

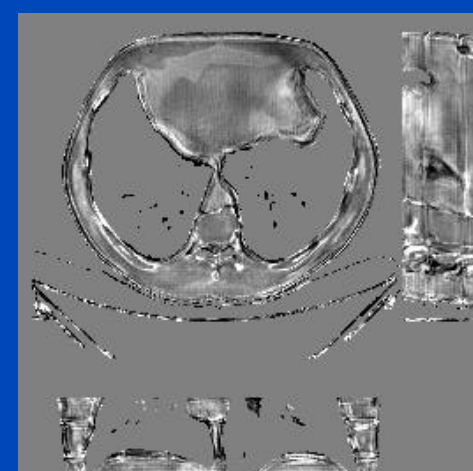

C = 0%
W = 40%

J. Maier, E. Eulig, S. Sawall, and M. Kachelrieß. Real-time patient-specific CT dose estimation using a deep convolutional neural network, Proc. IEEE MIC 2018 and ECR Book of Abstracts 2019. *Best Paper within Machine Learning at ECR 2019!*

Conclusions on DDE

- DDE provides accurate dose predictions
  - for circle scans
  - for sequence scans
  - for partial scans (less than 360°)
  - for limited angle scans (less than 180°)
  - for spiral scans
  - for different tube voltages
  - for scans with and without bowtie filtration
  - for scans with tube current modulation
- In practice it may therefore be not necessary to perform separate training runs for these cases.
- Thus, accurate real-time patient dose estimation may become feasible with DDE.

J. Maier, E. Eulig, S. Sawall, and M. Kachelrieß. Real-time patient-specific CT dose estimation using a deep convolutional neural network, Proc. IEEE MIC 2018 and ECR Book of Abstracts 2019. *Best Paper within Machine Learning at ECR 2019!*

Reconstruct from 1 or 2 Projections

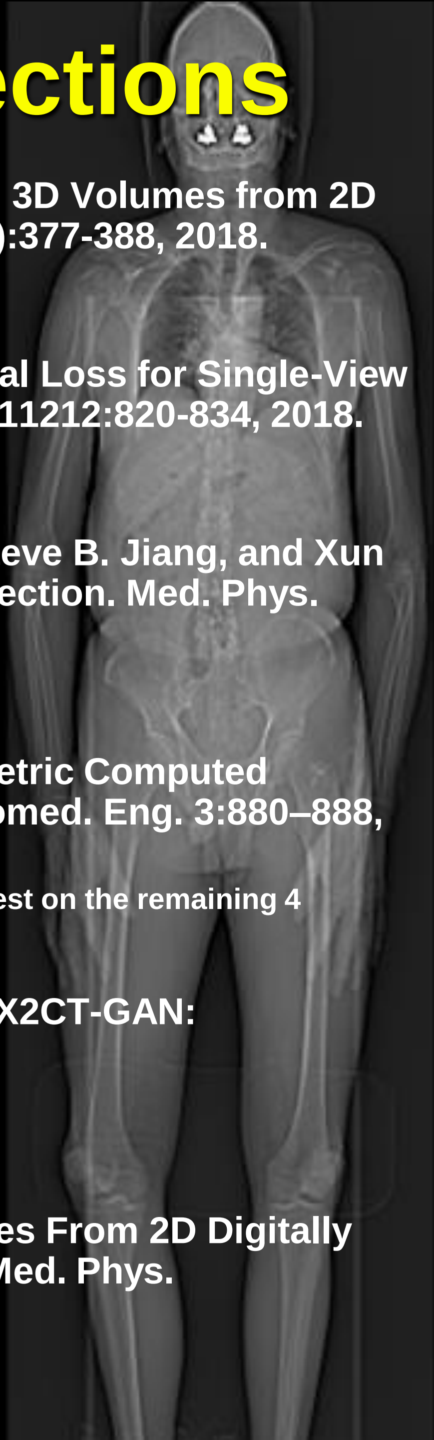

- P. Henzler, V. Rasche, T. Ropinski, and T. Ritschel. Single-image Tomography: 3D Volumes from 2D X-Rays: 3D Volumes from 2D Cranial X-Rays. Computer Graphics Forum. 37(2):377-388, 2018.
  – *N*=1, mainly sculls in air but also mouse with soft tissue
  – modified U-Net without reducing the number of features in the decoder (2D -> 3D)
- Li Jiang, Shaoshuai Shi, Xiaojuan Qi, and Jiaya Jia. GAL: Geometric Adversarial Loss for Single-View 3D-Object Reconstruction. In: ECCV 2018 Lecture Notes in Computer Science 11212:820-834, 2018.
  – *N*=1, object shapes from photography
  – GAN-type network
- Yuan Xu, Hao Yan, Luo Ouyang, Jing Wang, Linghong Zhou, Laura Cervino, Steve B. Jiang, and Xun Jia. A Method for Volumetric Imaging in Radiotherapy using Single X-Ray Projection. Med. Phys. 42(5):2498-2509, 2015
  – *N*=1. Derives MVFs from an x-ray projection that are then applied to a 3D CBCT volume
  – Sparse learning
- Liyue Shen, Wei Zhao, and Lei Xing. Patient-Specific Reconstruction of Volumetric Computed Tomography Images from a Single Projection View via Deep Learning. Nat. Biomed. Eng. 3:880–888, 2019.
  – *N*=1. Training and validation in the same patient. Example 1: train on 6 phases of 4D CT and test on the remaining 4 phases. Example 2: train on 4D CT of day 1 and test on 4D CT of day 2.
  2D encoder CNN, 2D->3D FCN, 3D decoder CNN.
- Xingde Ying, Heng Guo, Kai Ma, Jian Wu, Zhengxin Weng, and Yefeng Zheng. X2CT-GAN: Reconstructing CT from Biplanar X-Rays with Generative Adversarial Networks. arXiv:1905.06902v1, May 2019
  – *N*=2. Thorax cases
  – GAN with U-Net-type generator whose skips are backprojections.
- Diogo F. Almeida, Patricio Astudillo, and Dirk Vandermeulen. 3D Image Volumes From 2D Digitally Reconstructed X-Rays: A Deep Learning Approach In Lower Limb CT-Scans. Med. Phys. 48:published online, 2021.
  – *N*=2. Lower limb DRRs.
  – Based on Henzler et al. (see above).

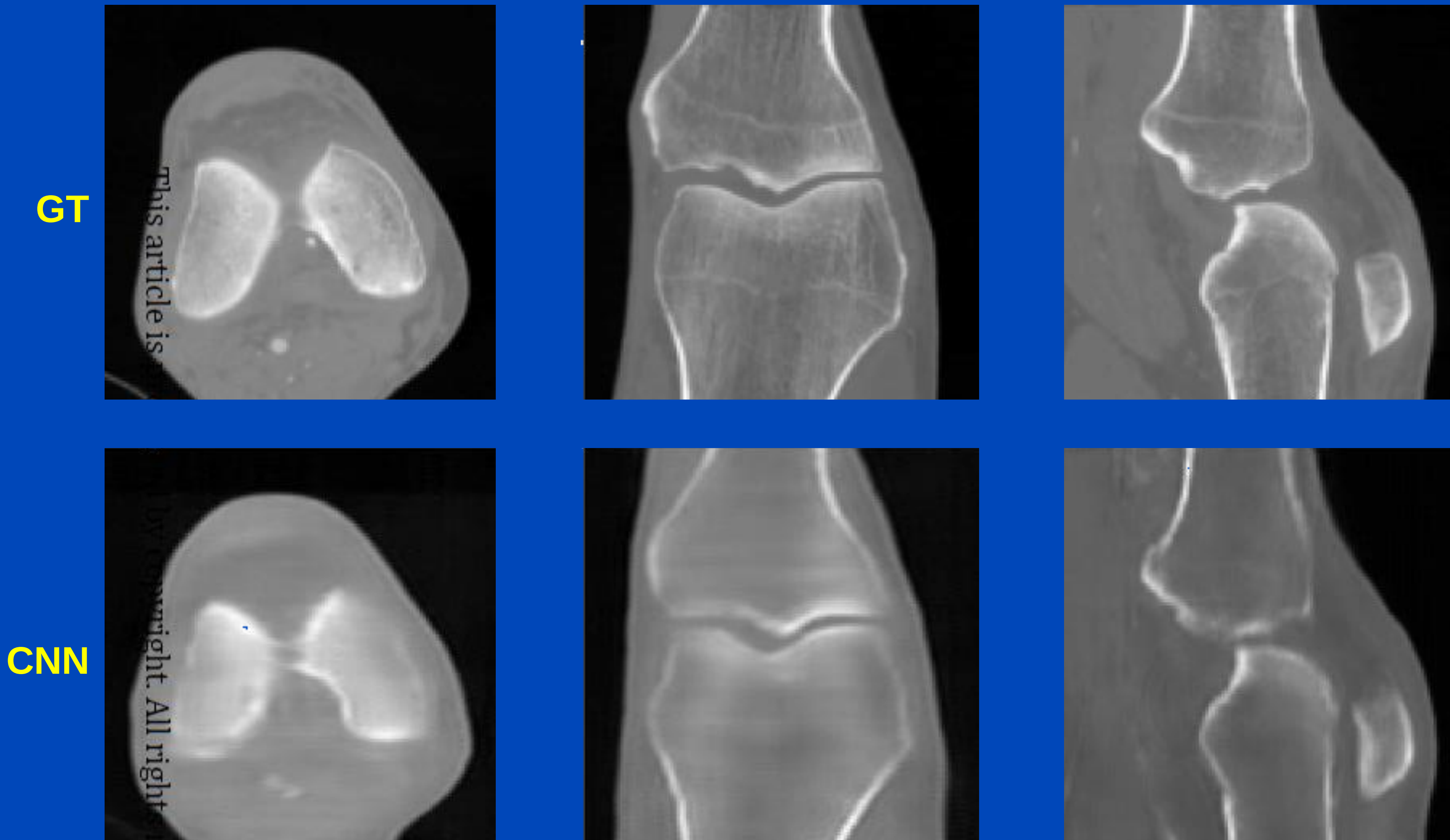

Almeida, Astudillo, and Vandermeulen. 3D Image Volumes From 2D Digitally Reconstructed X-Rays: A Deep Learning Approach In Lower Limb CT-Scans. Med. Phys. 48:published online, 2021.

What for?

- Avoid CT scans if only coarse 3D information is required.
- Real-time guidance in RT or in intervention: Generate 4D volumes from fluoroscopy (a series of x-ray CT image)
- Niche applications
  - Assess location and size of organs from just one or two x-ray images
  - Patient position verification
  - …
- Perform patient-specific tube current modulation (next slides).

Patient Risk-Minimizing Tube Current Modulation

1. **Coarse reconstruction from two scout views**
   – E.g. X. Ying, et al. X2CT-GAN: Reconstructing CT from biplanar x-rays with generative adversarial networks. CVPR 2019.

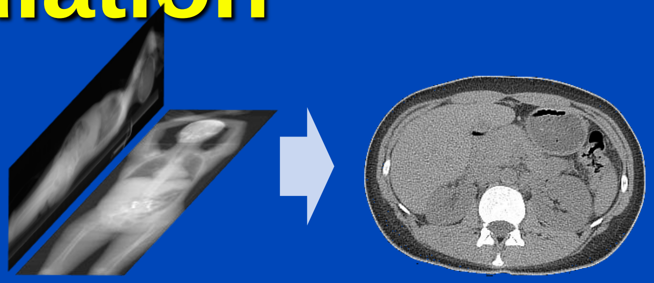

2. **Segmentation of radiation-sensitive organs**
   – E.g. S. Chen, M. Kachelrieß et al., Automatic multi-organ segmentation in dual-energy CT (DECT) with dedicated 3D fully convolutional DECT networks. Med. Phys. 2019.

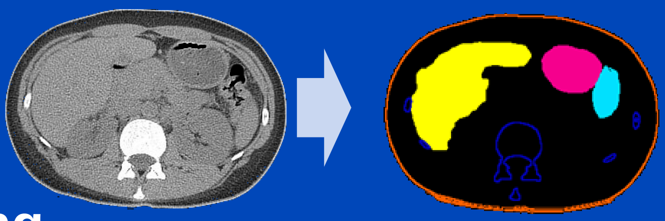

3. **Calculation of the effective dose per view using the deep dose estimation (DDE)**
   – J. Maier, E. Eulig, S. Dorn, S. Sawall and M. Kachelrieß. Real-time patient-specific CT dose estimation using a deep convolutional neural network. IEEE Medical Imaging Conference Record, M-03-178: 3 pages, Nov. 2018.

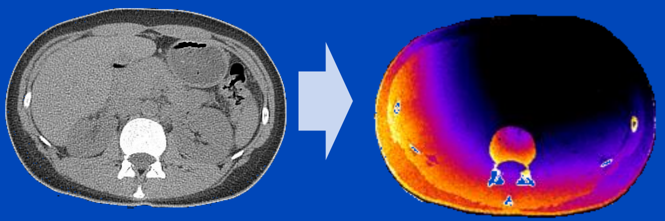

4. **Determination of the tube current modulation curve that minimizes the radiation risk**
   – L. Klein, J. Maier, C. Liu, A. Maier, M. Lell, and M. Kachelrieß. Patient radiation risk–minimizing tube current modulation for diagnostic CT. Submitted to Med. Phys., 2021.

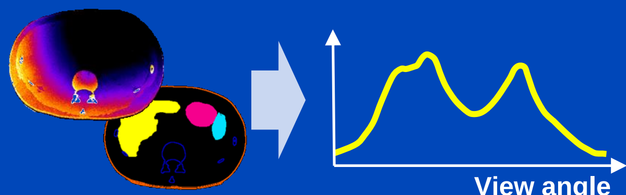

Remainder 0.12
Bone surface 0.01
Brain 0.01
Breast 0.12
Colon 0.12
Red Bone Marrow 0.12
Salivary glands 0.01
Esophagus 0.04
Liver 0.04
Lung 0.12
Skin 0.01
Stomach 0.12
Gonads 0.08
Thyroid 0.04
Bladder 0.04

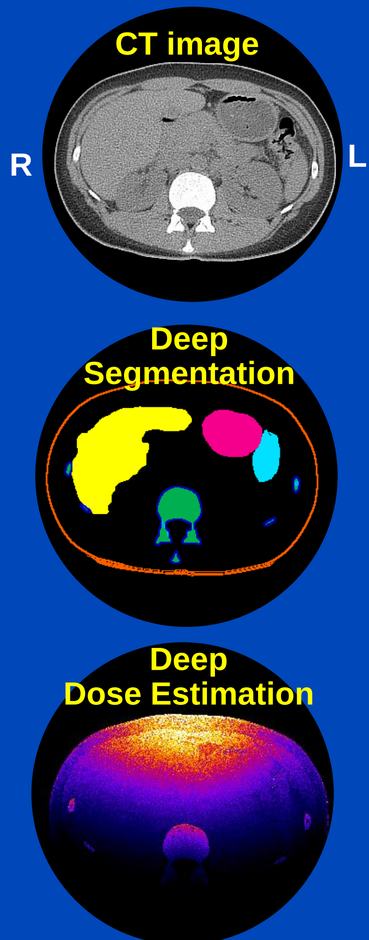

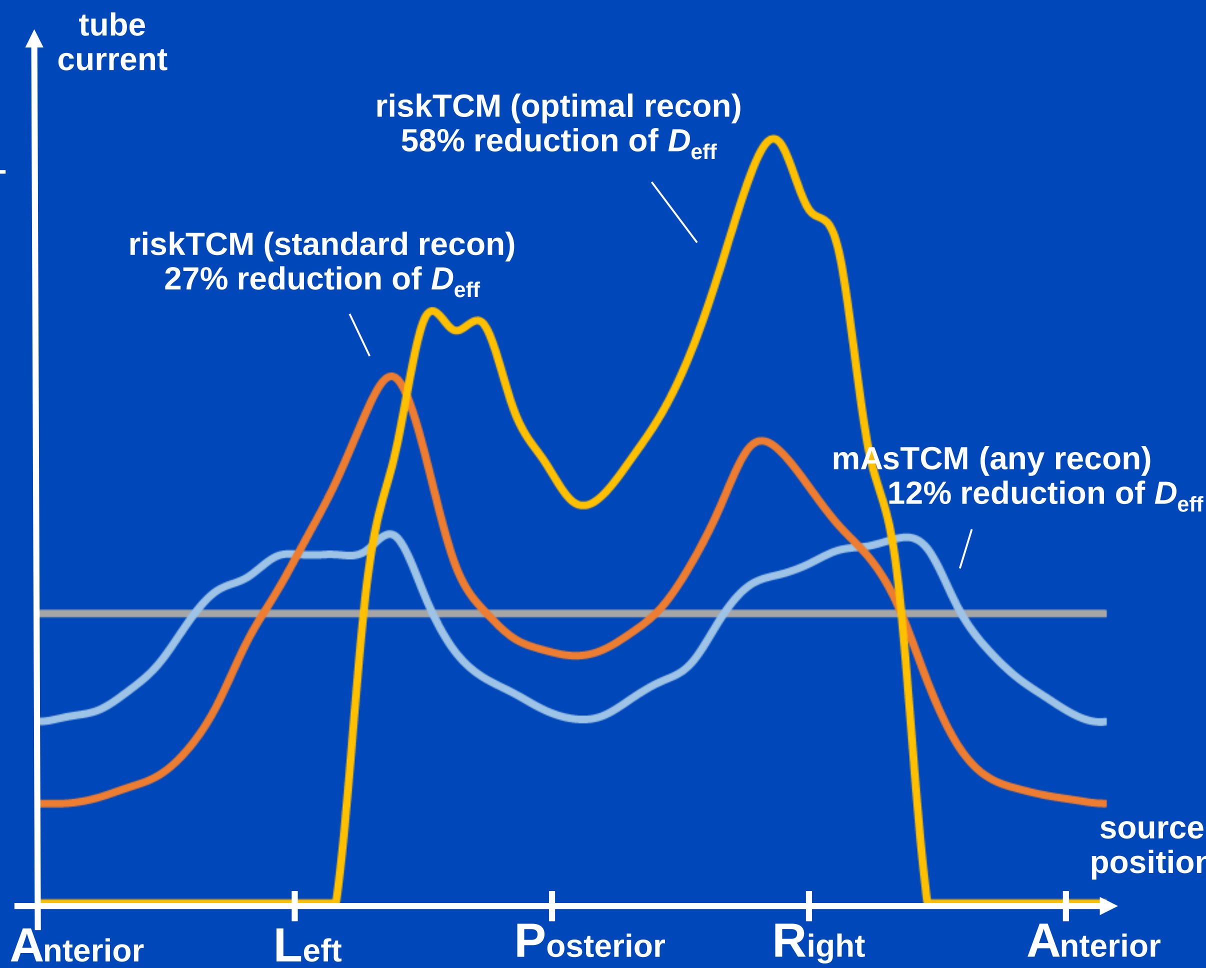

Patient 03 - Neck

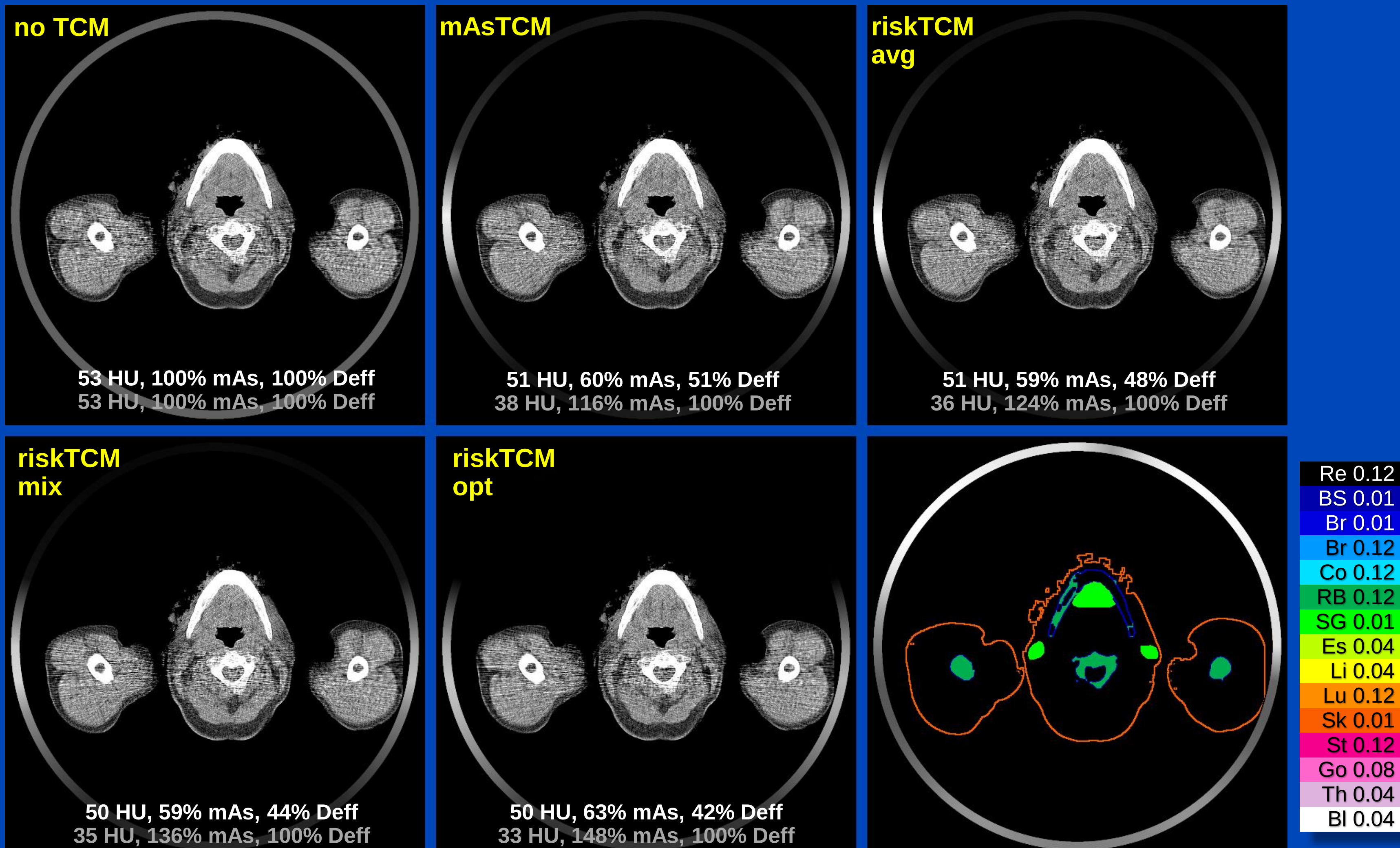

C = 25 HU, *W* = 400 HU

Patient 03 - Pelvis

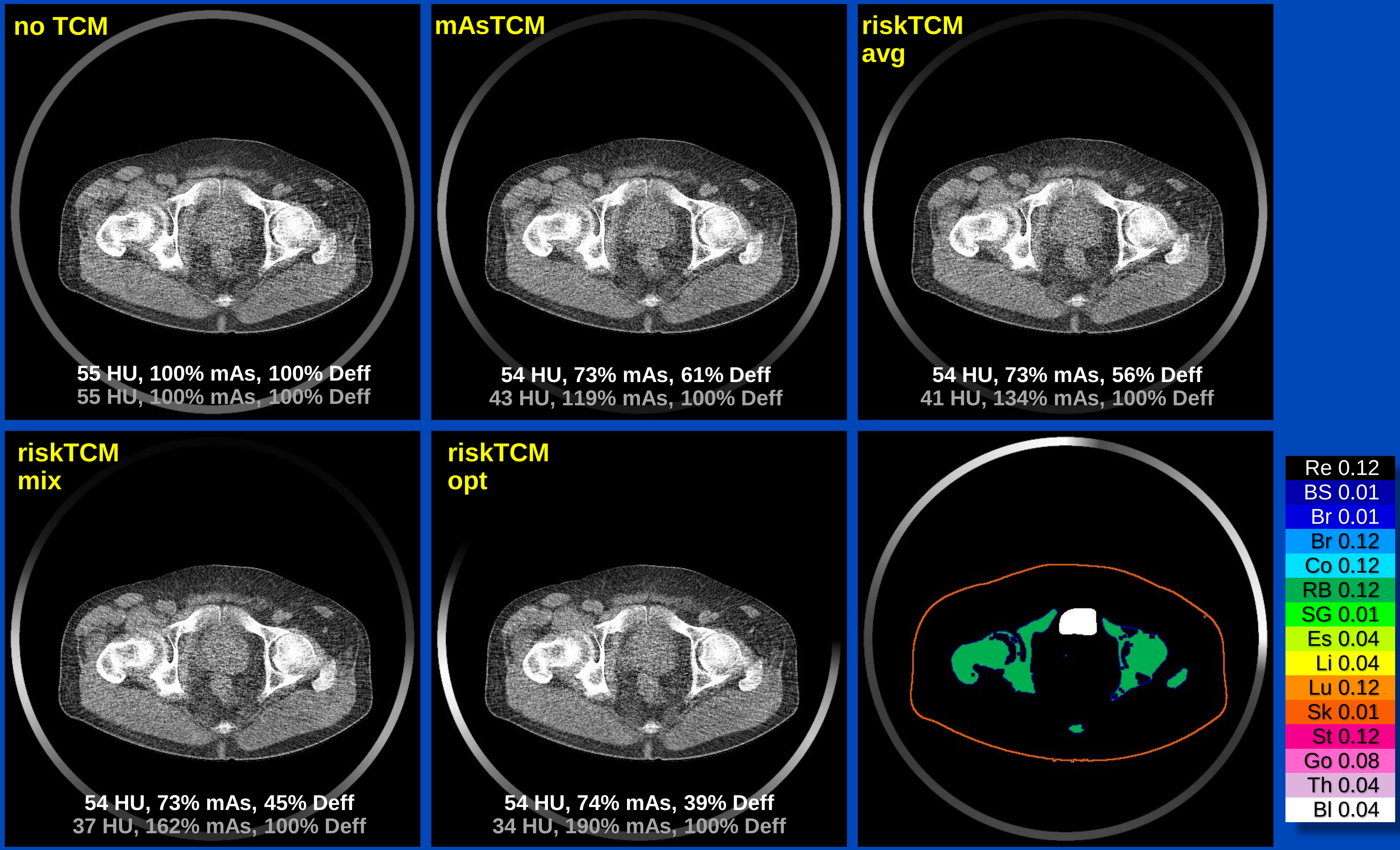

C = 25 HU, *W* = 400 HU

Patient 04 - Abdomen

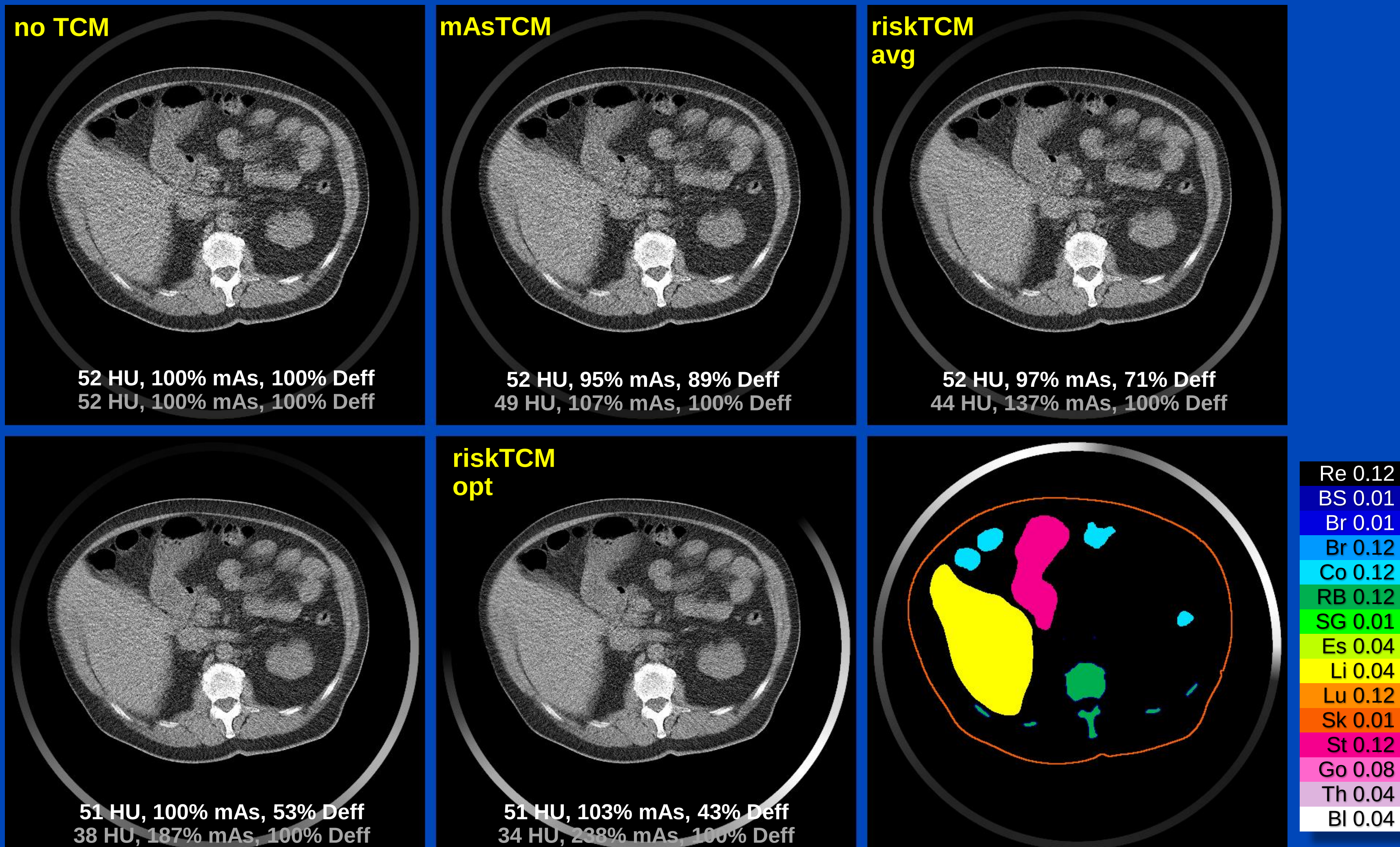

C = 25 HU, *W* = 400 HU

Part 4:

Image Reconstruction

Variational Network-Based Image Reconstruction

$$C(\boldsymbol{f}) = \|\boldsymbol{X}\cdot\boldsymbol{f}-\boldsymbol{p}\|_{\boldsymbol{W}}^2 + R(\boldsymbol{f})$$

$$\boldsymbol{\nabla} C(\boldsymbol{f}) = \boldsymbol{X}^{\mathrm{T}}\cdot\boldsymbol{W}\cdot(\boldsymbol{X}\cdot\boldsymbol{f}-\boldsymbol{p}) + \boldsymbol{\nabla} R(\boldsymbol{f})$$

$$\boldsymbol{f}^{(t+1)} = \boldsymbol{f}^{(t)} - \lambda\boldsymbol{\nabla} C(\boldsymbol{f}^{(t)})$$

Highly simplified example. Varnets work for a much wider class of cost functions whose NN-based minimization is motivated by the primal dual approach.

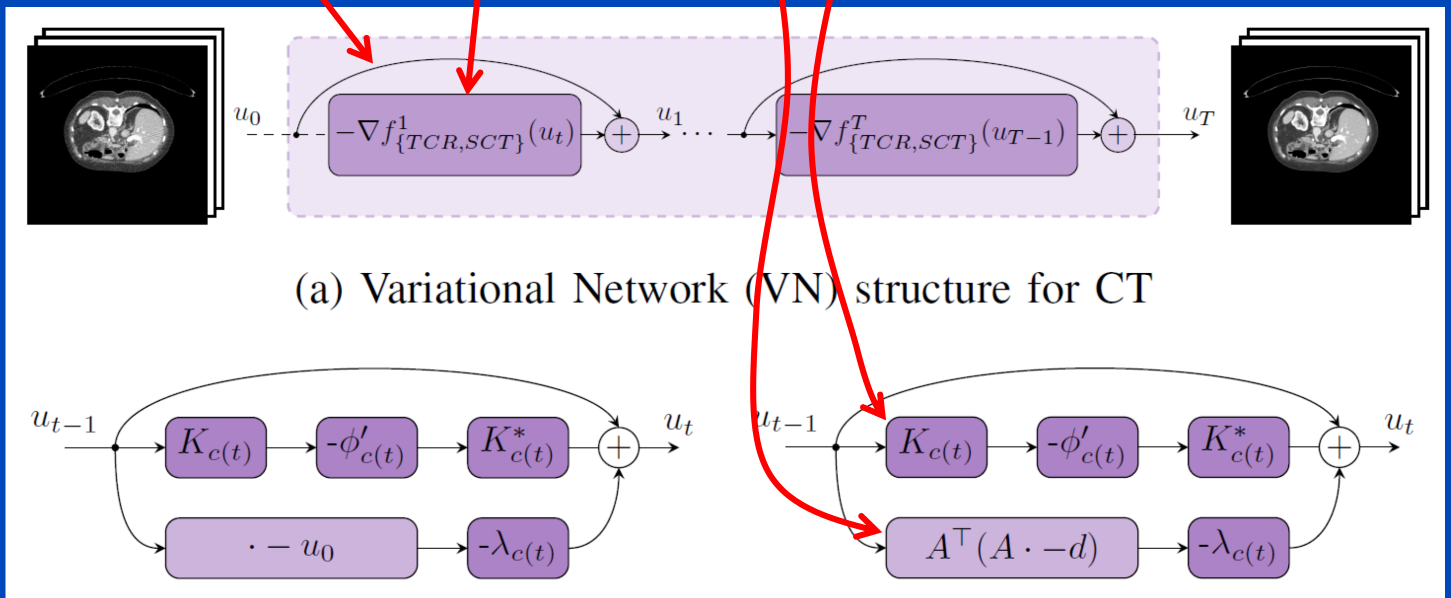

(a) Variational Network (VN) structure for CT

(b) VU for CT denoising

(c) VU for CT reconstruction

E. Kobler, R. Otazo et al. Variational network learning for low-dose CT. Proc. 5th CT-Meeting:430-434, 2018.

full dose

1/4 dose

1/6 dose

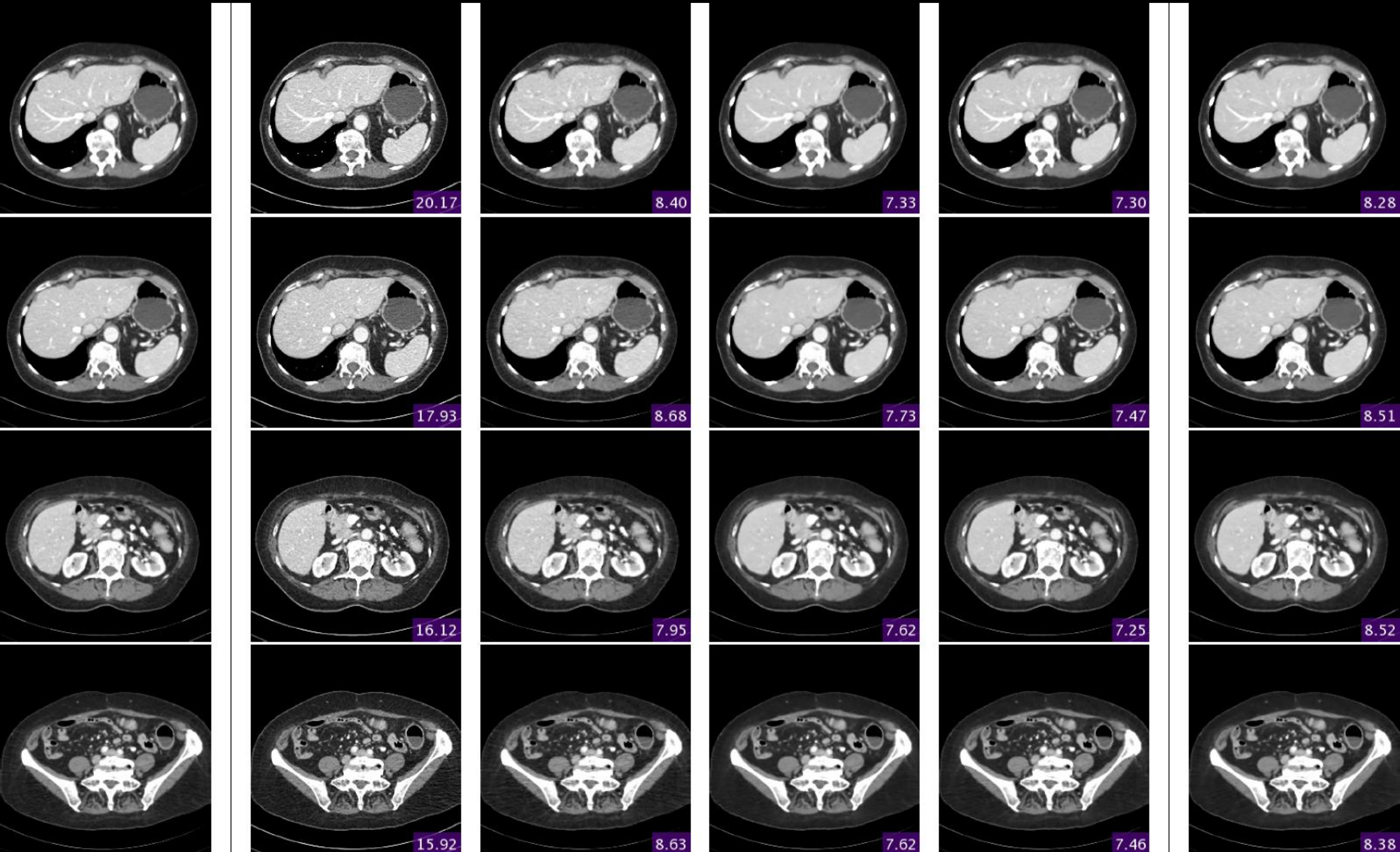

(a) full-dose | (b) SAFIRE | (c) TV | (d) TCR | (e) SCT | (f) SCT

tube current reduction SAFIRE | sparse views TV | tube current reduction varnet | sparse views varnet | sparse views varnet

Part 5:

Motion Compensation (MoCo)

Deep Cardiac Motion Compensation

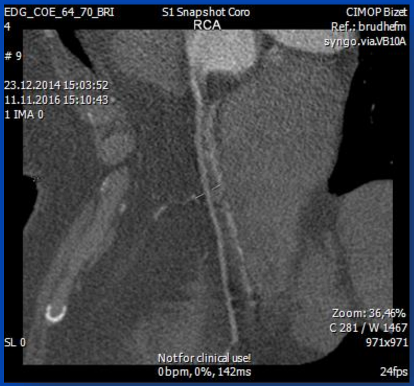

???

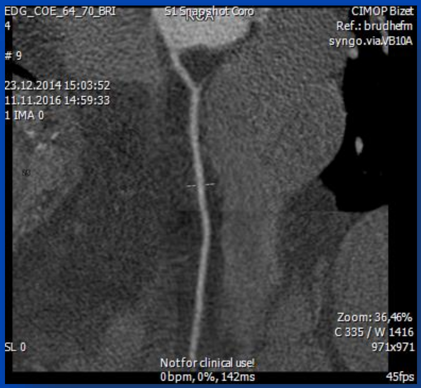

Deep PAMoCo

Network architecture

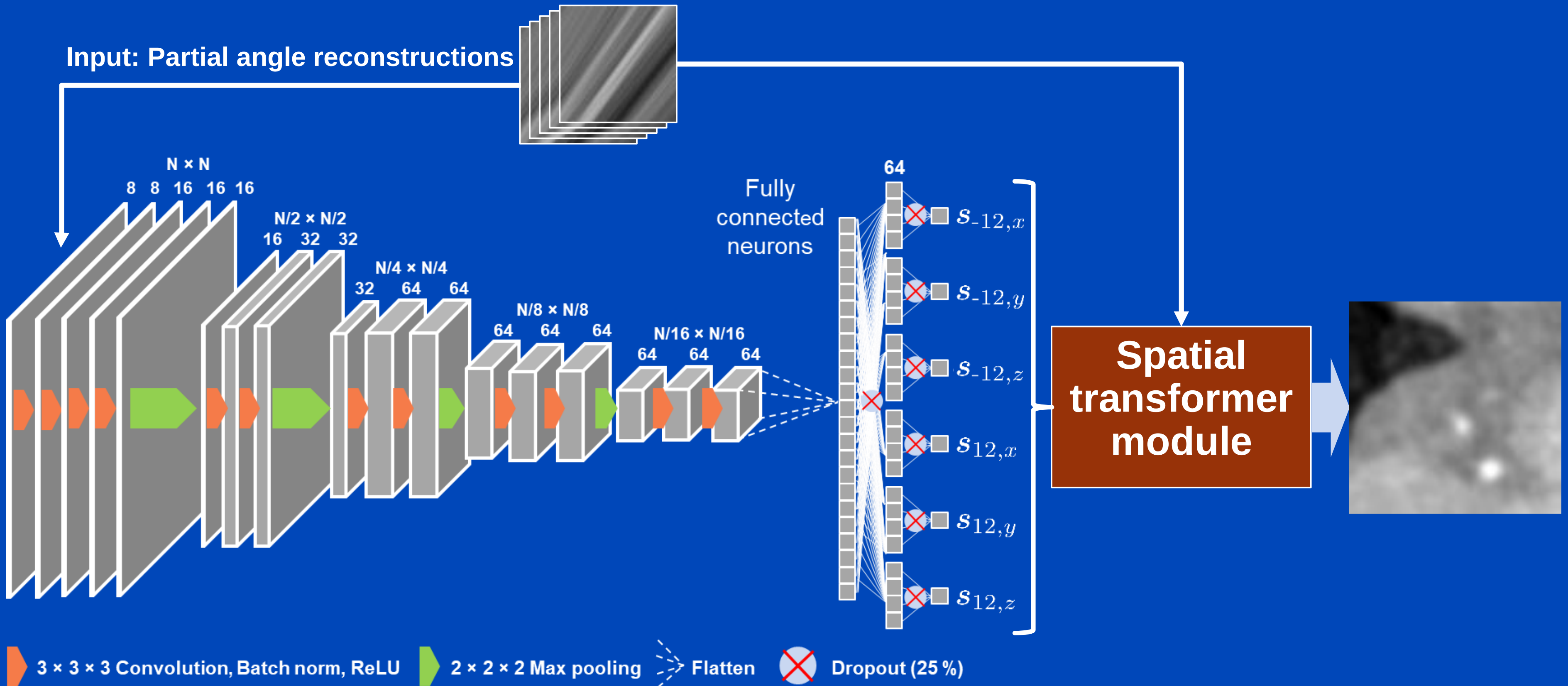

J. Maier, S. Lebedev, J. Erath, E. Eulig, S. Sawall, E. Fournié, K. Stierstorfer, M. Lell, and M. Kachelrieß. Deep learning-based coronary artery motion estimation and compensation for short-scan cardiac CT. Med. Phys. 48, in press, 2021.

J. Maier, S. Lebedev, E. Eulig, S. Sawall, E. Fournié, K. Stierstorfer, and M. Kachelrieß. Coronary artery motion compensation for short-scan cardiac CT using a spatial transformer network. Conference Program of the 6th International CT-Meeting, August 2020.

dkfz.

Results

Measurements, patient 1

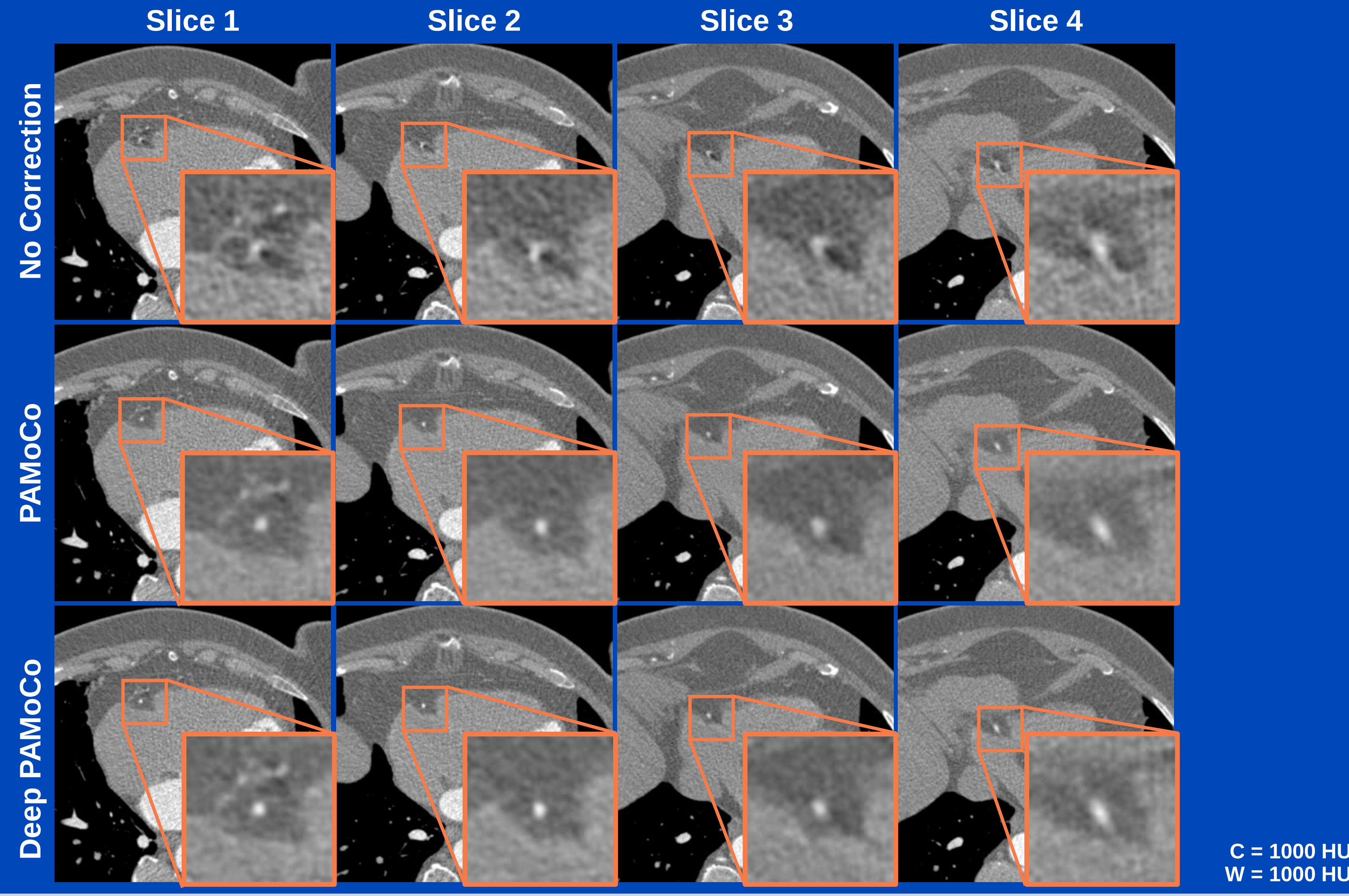

J. Maier, S. Lebedev, E. Eulig, S. Sawall, E. Fournié, K. Stierstorfer, and M. Kachelrieß. Coronary artery motion compensation for short-scan cardiac CT using a spatial transformer network. Conference Program of the 6th International CT-Meeting, August 2020.

Results

Measurements, patient 2

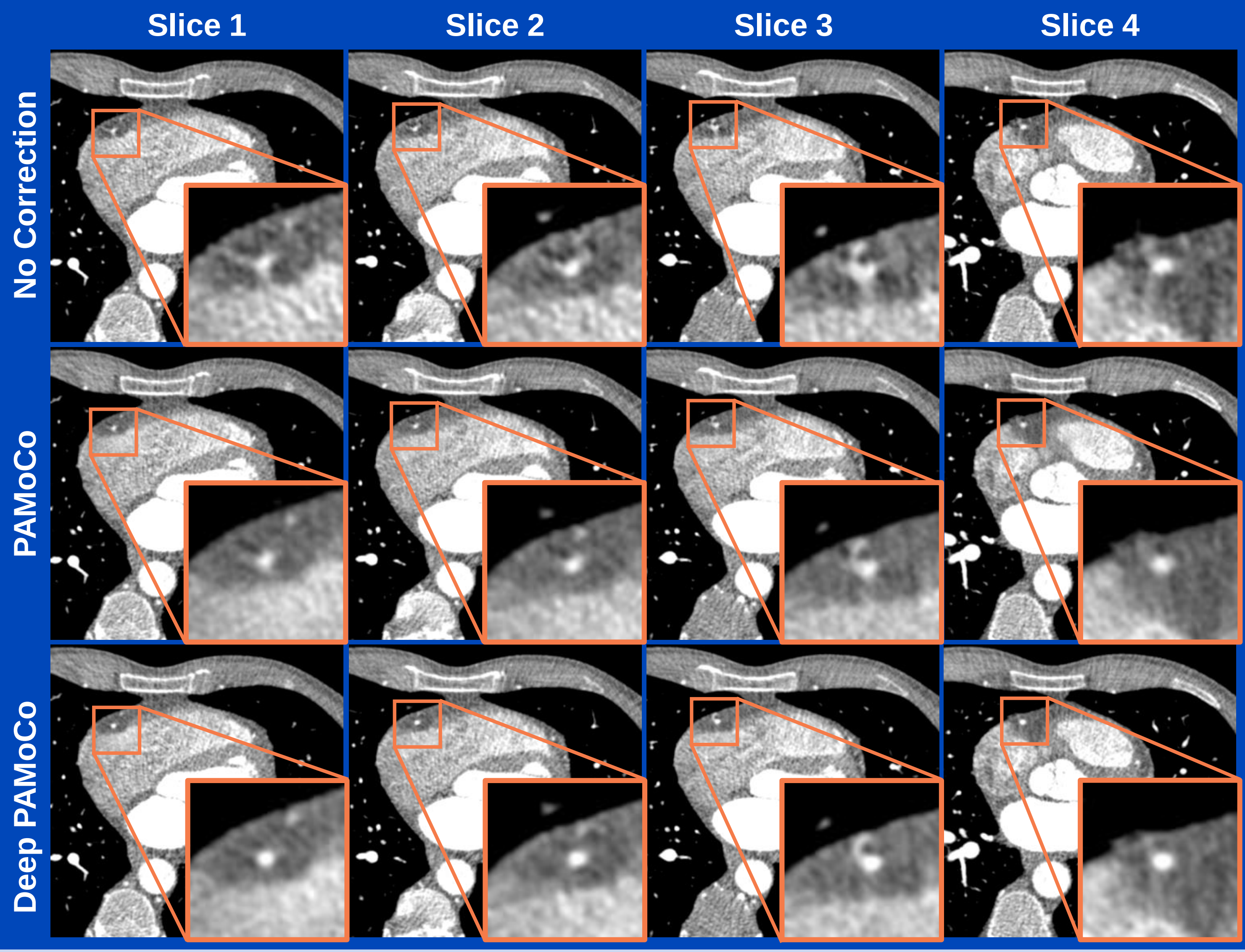

C = 1000 HU
W = 1000 HU

J. Maier, S. Lebedev, E. Eulig, S. Sawall, E. Fournié, K. Stierstorfer, and M. Kachelrieß. Coronary artery motion compensation for short-scan cardiac CT using a spatial transformer network. Conference Program of the 6th International CT-Meeting, August 2020.

Results

Measurements, patient 3

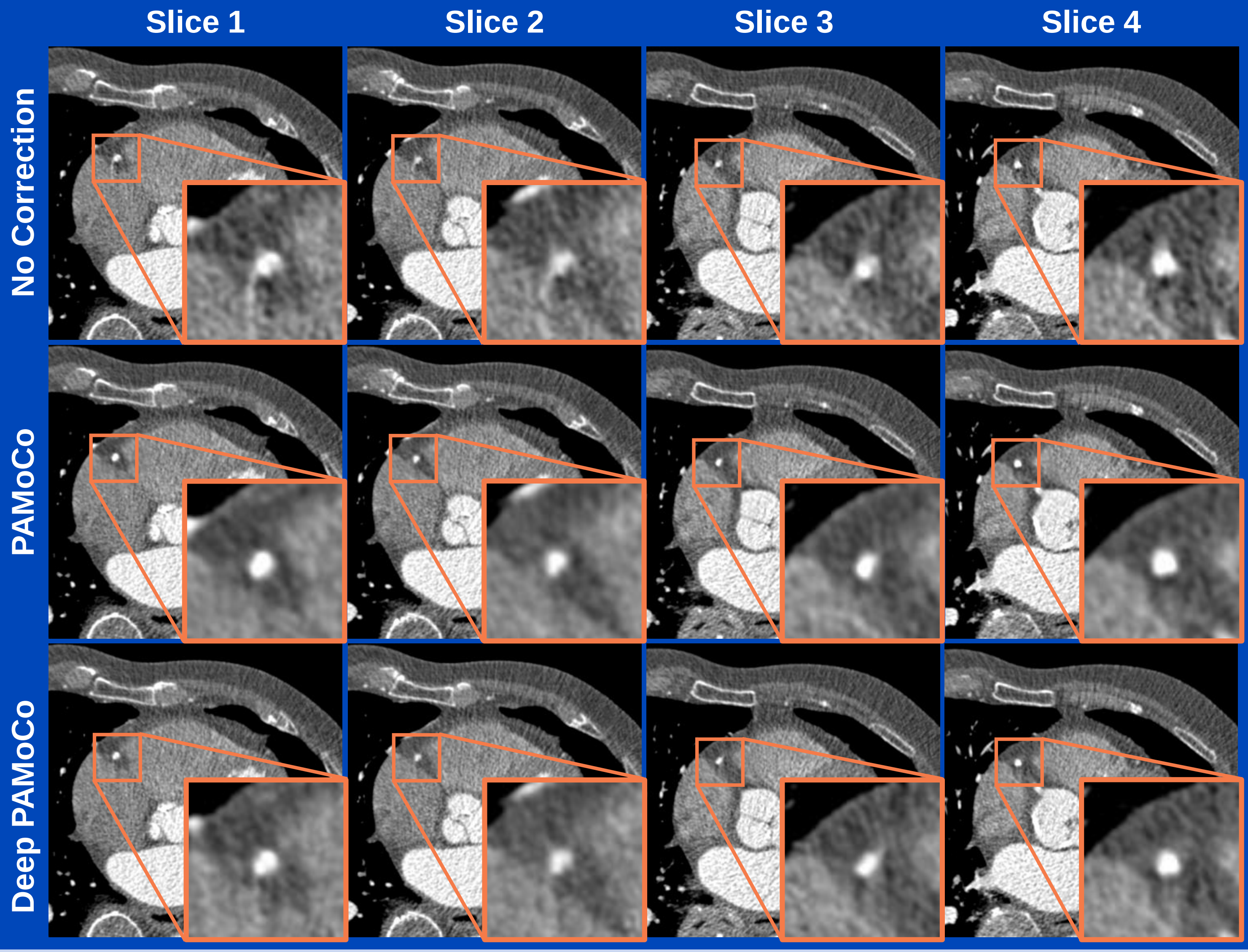

C = 1100 HU
W = 1000 HU

Intervention goes Deep!

Deep DSA

???

Without mask?

Methods
General principle

Conventional DSA

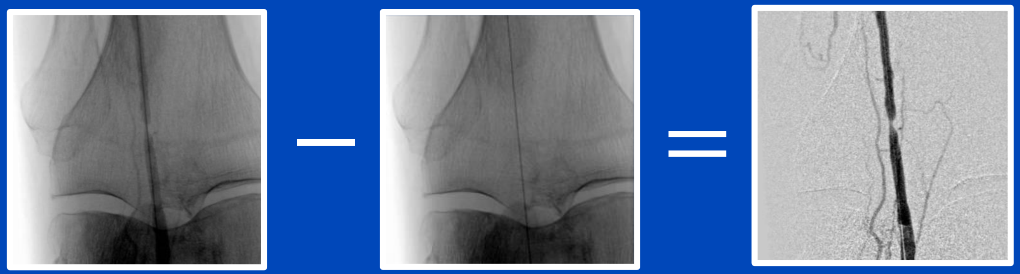

I_t I_0 $\tilde{I}_t$

Deep DSA

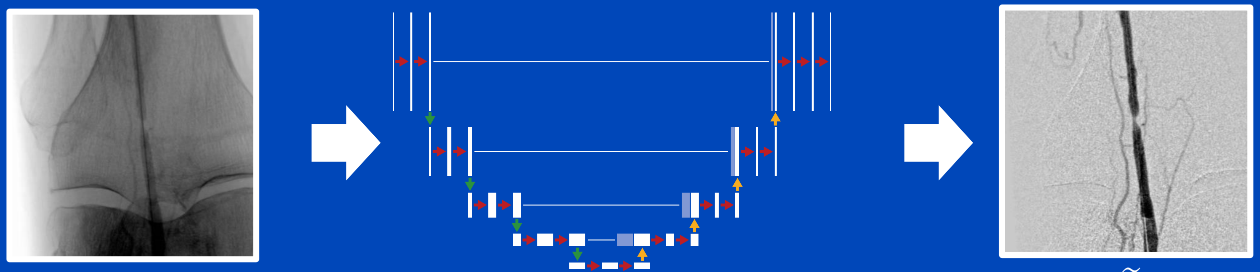

I_t $\tilde{I}_t$

- **Train on static cases where ground truth is conventional DSA**

E. Eulig, M. Kachelrieß, et al. "Learned digital subtraction angiography (Deep DSA): method and application to lower extremities". Proc. SPIE 11072, 15th International Meeting on Fully Three-Dimensional Image Reconstruction, 1107223:1-4, May 2019.

Results

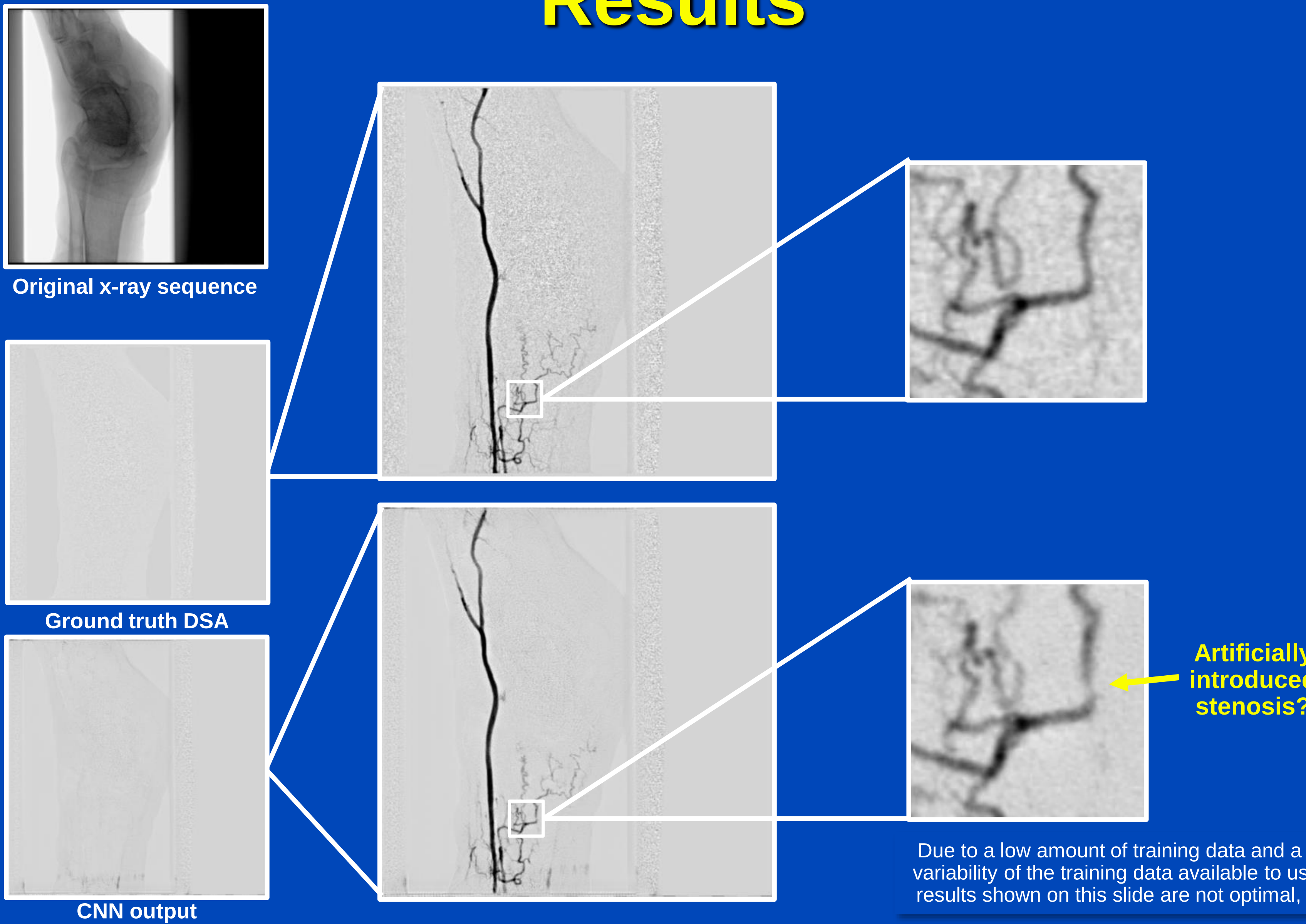

Due to a low amount of training data and a low variability of the training data available to us the results shown on this slide are not optimal, yet.

E. Eulig, M. Kachelrieß, et al. "Learned digital subtraction angiography (Deep DSA): method and application to lower extremities". Proc. SPIE 11072, 15th International Meeting on Fully Three-Dimensional Image Reconstruction, 1107223:1-4, May 2019.

Deep DSA

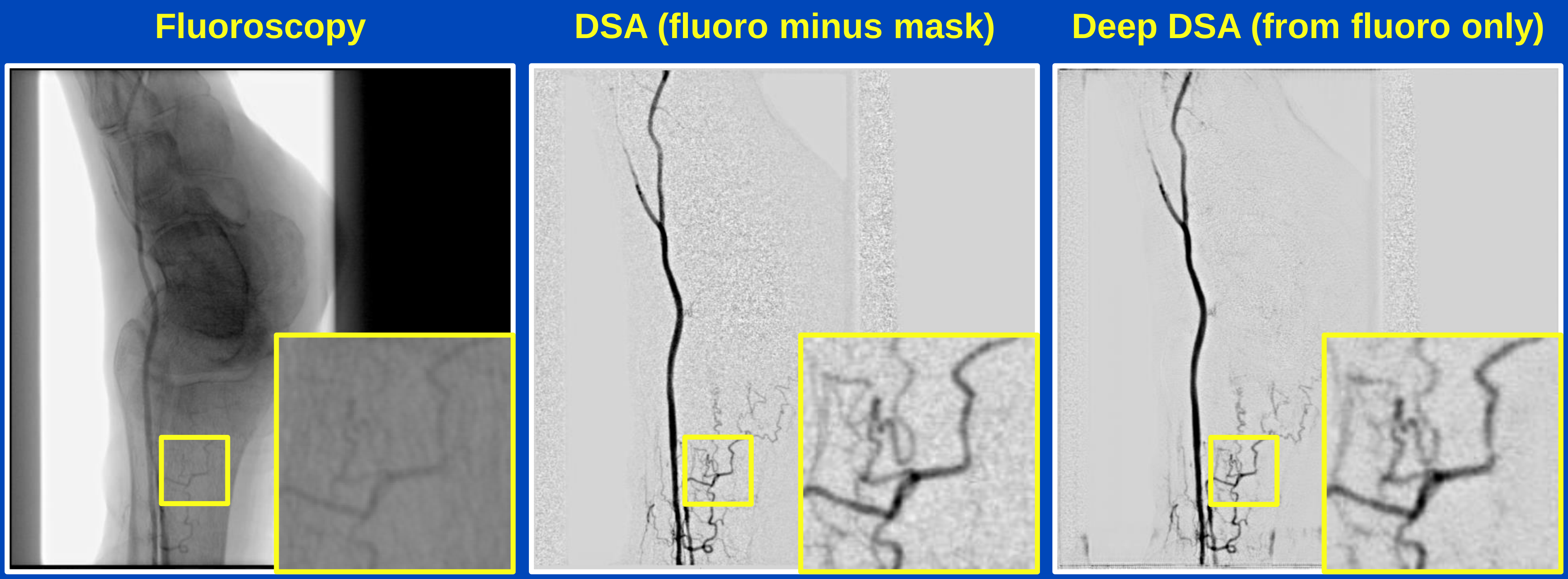

Due to a low amount of training data and a low variability of the training data available to us the results shown on this slide are not optimal, yet.

E. Eulig, M. Kachelrieß, et al. "Learned digital subtraction angiography (Deep DSA): method and application to lower extremities". Proc. SPIE 11072, 15th International Meeting on Fully Three-Dimensional Image Reconstruction, 1107223:1-4, May 2019.

Results
Bolus chase study

Dynamic fluoroscopy

Conventional DSA

Conventional DSA infeasible due to C-arm motion

Deep DSA

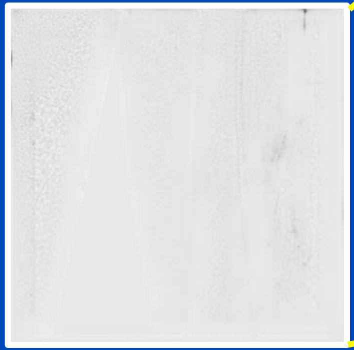

Deep DSA at t $= t_a$

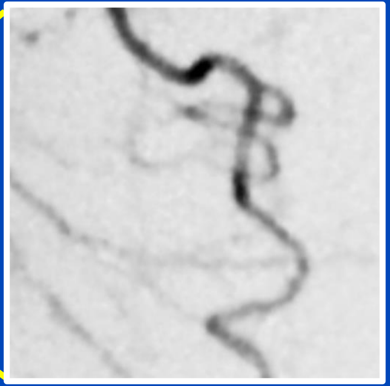

Deep DSA at t $= t_a$

E. Eulig, M. Kachelrieß, et al. "Learned digital subtraction angiography (Deep DSA): method and application to lower extremities". Proc. SPIE 11072, 15th International Meeting on Fully Three-Dimensional Image Reconstruction, 1107223:1-4, May 2019.

Deep 3D+T Fluoroscopy

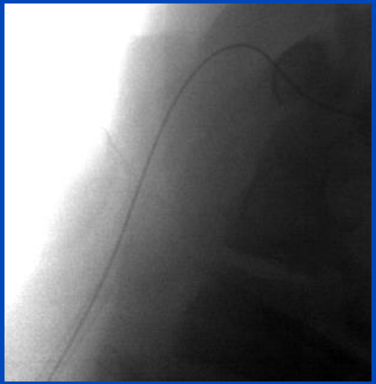

???

At 2D+T dose?

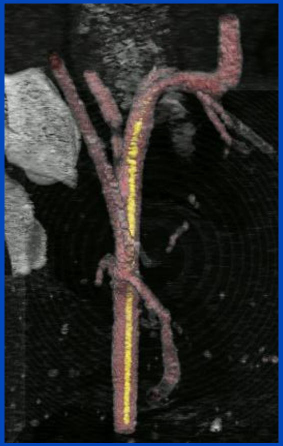

Deep 3D+T Tomographic Fluoroscopy

either 2D+T fluoroscopy

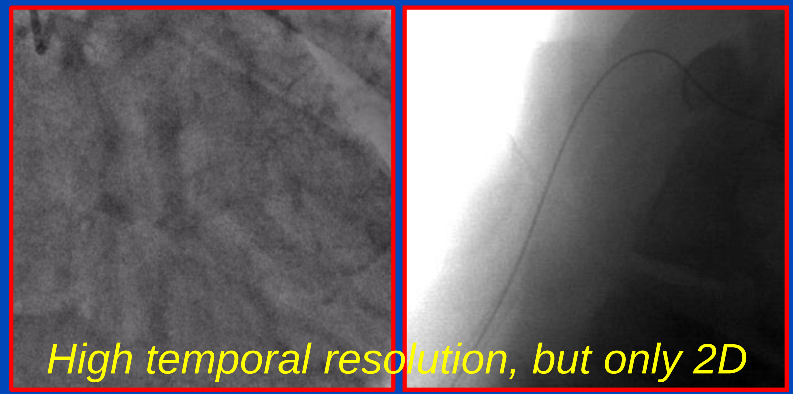

or 3D tomography

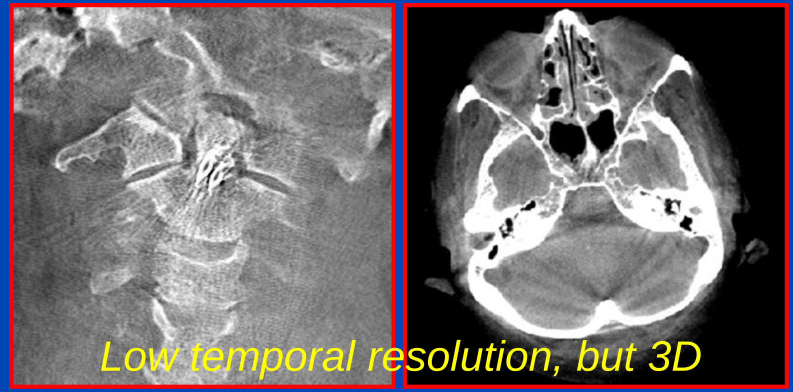

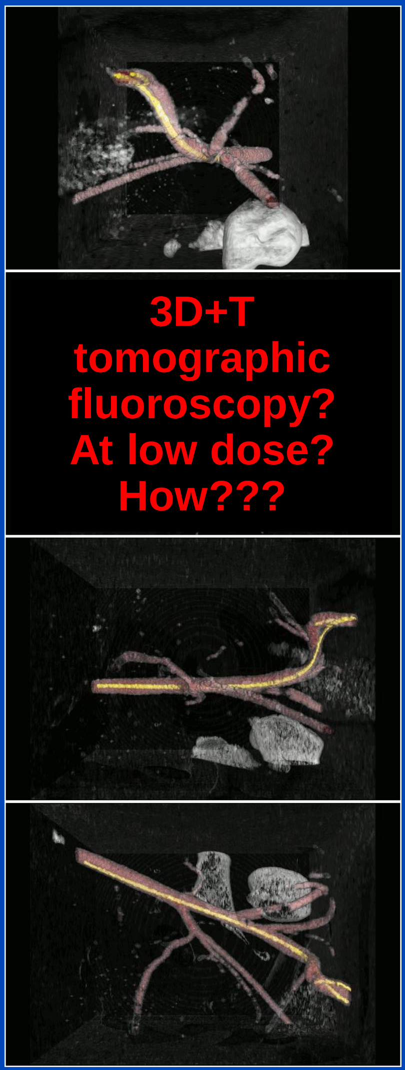

How to Realize 3D+T Fluoroscopy

- Low dose by:
  - Low tube current
  - Very few projections (pulsed mode)
- Advantages of intervention guidance:
  - Repetitive scanning of the same body region: changes are sparse.
  - Interventional materials are fine structures (few voxels) of high contrast (metal).

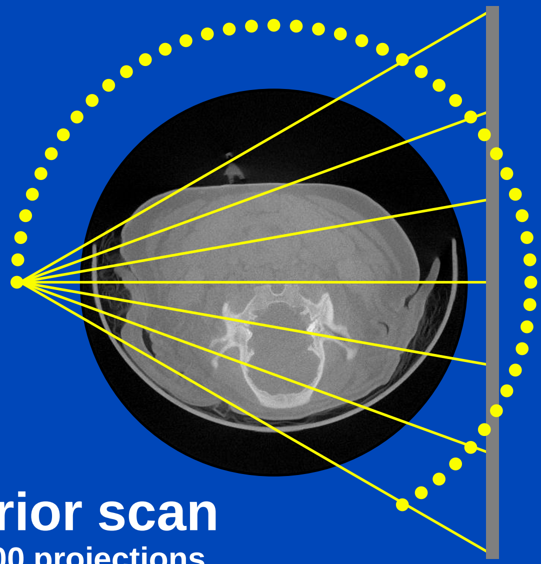

Prior scan
400 projections

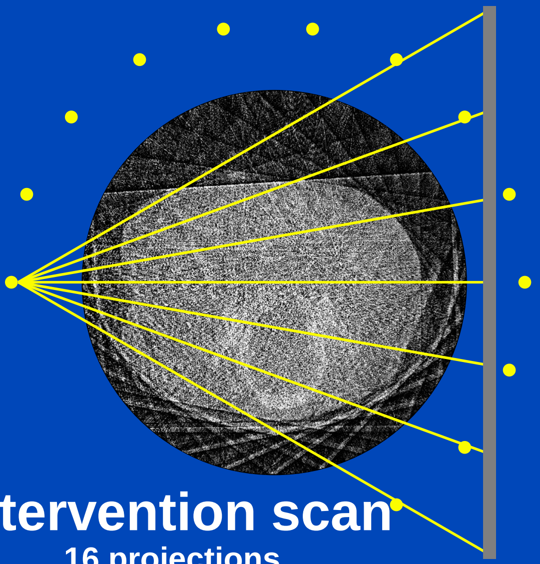

Intervention scan
16 projections

Experimental setup

B. Flach, J. Kuntz, M. Brehm, R. Kueres, S. Bartling, and M. Kachelrieß. "Low dose tomographic fluoroscopy: 4D intervention guidance with running prior.", Med. Phys. 40:101909, 11 pages, October 2013.

dkfz.

3D+T Image Guidance at 2D+T Dose

Stent Expansion in the Carotis of a Pig with Angio Roadmap Overlay

Iterative reconstruction using prior knowledge inside!

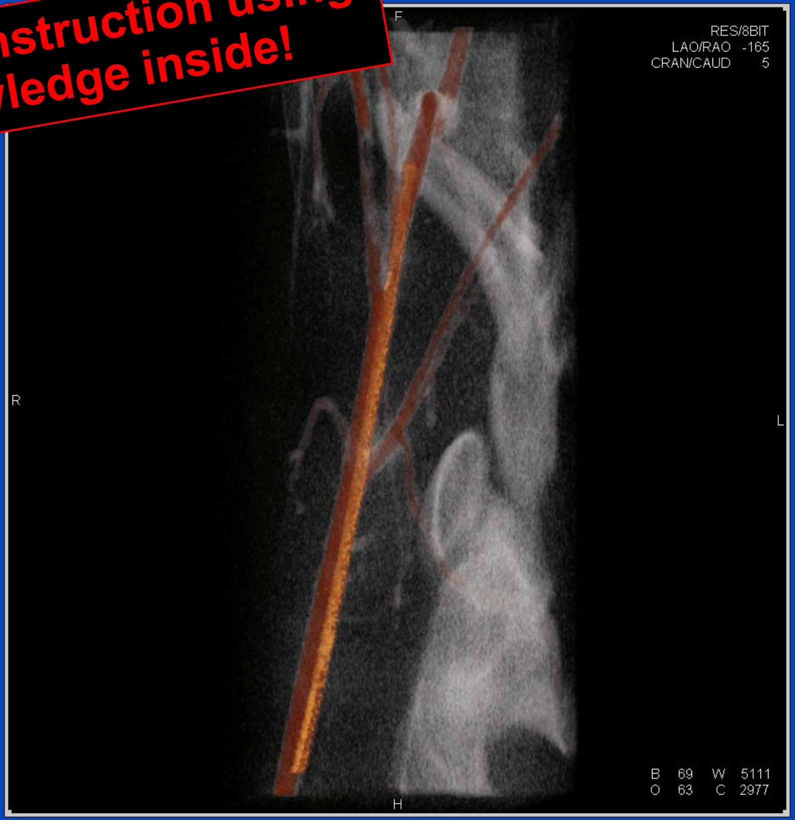

Dose of the yet unoptimized approach: 20 bis 50 µGy/s.

This work was awarded the intervention award 2013 of the German Society of Neuroradiology (DGNR).
This work was further selected as the Editor's Pick for the Medical Physics Scitation site.

3D+T Fluoroscopy at 2D+T Dose

Guide Wire in the Carotis of a Pig with Angio Roadmap Overlay

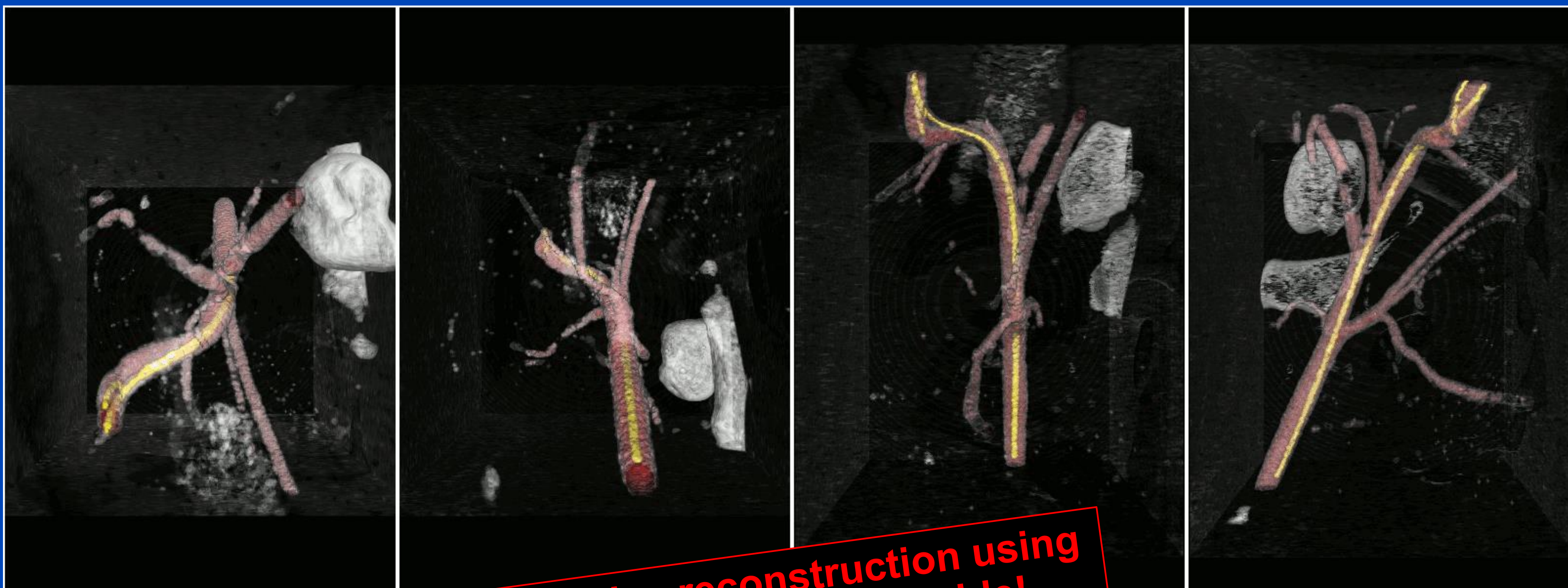

Iterative reconstruction using prior knowledge inside!

Dose of the yet unoptimized approach: 20 to 50 µGy/s. Obviously, 16 projections are too much.

New Method: 4 Projections Only!

Deep Tool Extraction (DTE), Feldkamp Recon (FDK), Deep Tool Reconstruction (DTR)

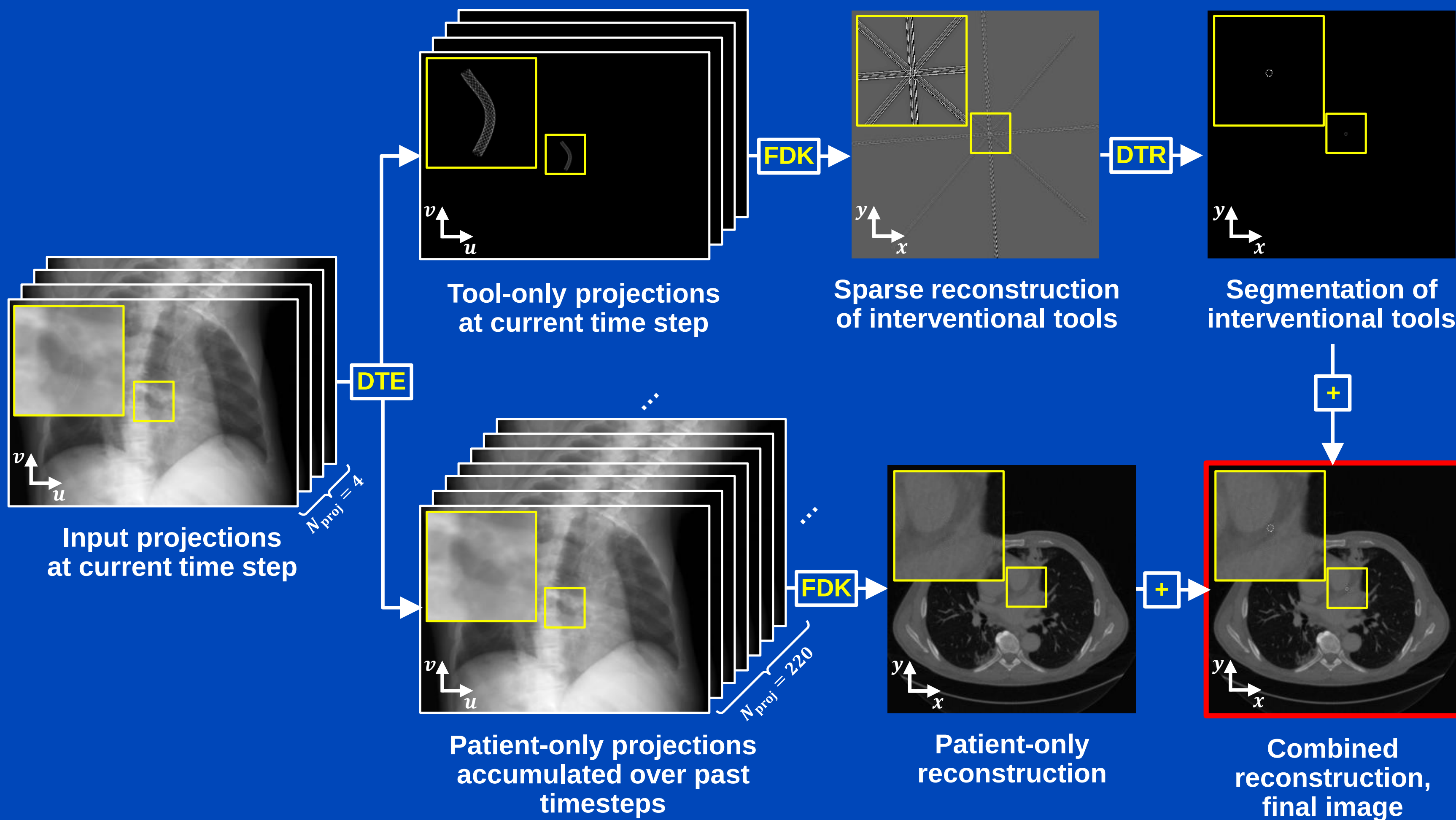

E. Eulig, J. Maier, N.R. Bennet, M. Knaup, K. Hörndler, A. Wang, and M. Kachelrieß. Deep learning-aided CBCT image reconstruction of interventional material from four x-ray projections. SPIE Medical Imaging Conference Record, 113121L:1-7, March 2020.

Zeego @ Stanford University

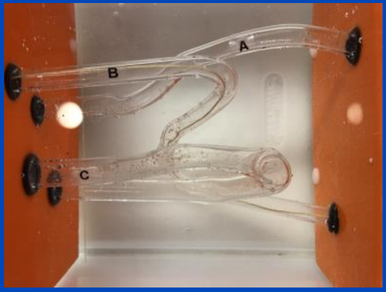

dkfz.

Zeego Measurements with Just 4 Projections

Ground truth (measurements from 400 projections)

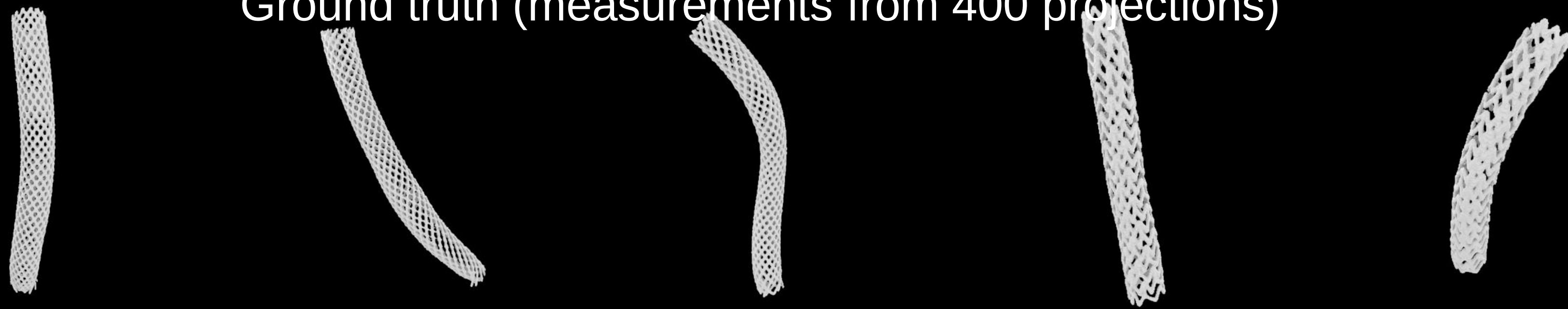

Neural network output (from just 4 projections)

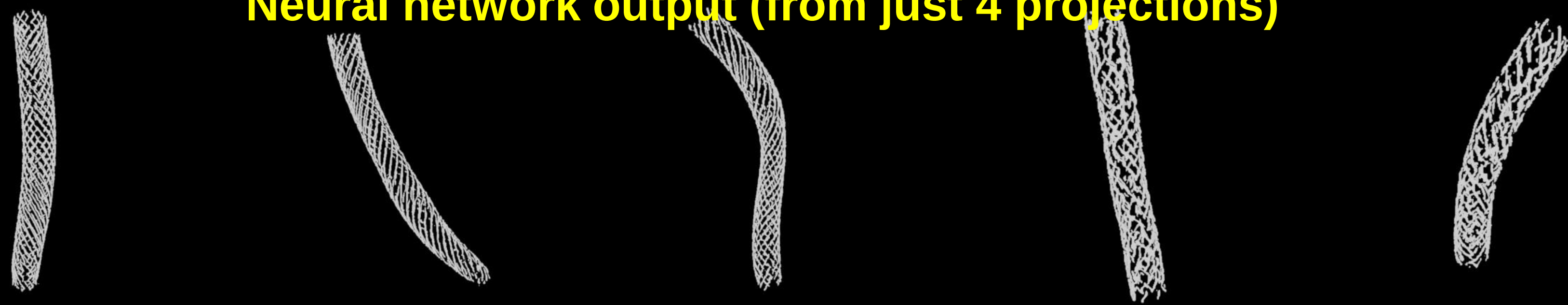

Loop through slices reconstructed from just 4 projections without AI:

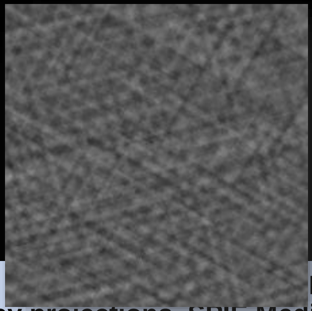

Stent examples:

E. Eulig, J. Maier, N.R. Bennet, M. Knaup, K. … M. Kachelrieß. Deep l… of interventional material from four x-ray projections. SPIE Medical Imaging Conference Record, 113121L:1-7, March 2020.

Thank You!

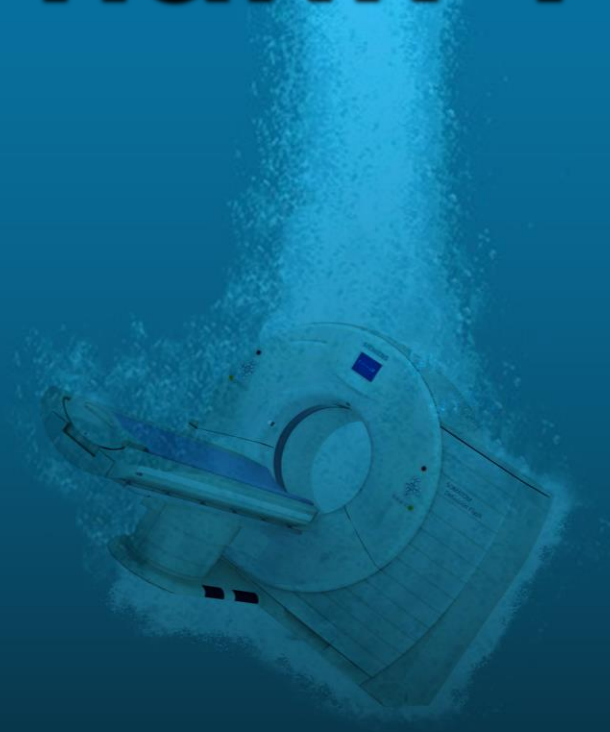

This presentation will soon be available at www.dkfz.de/ct.

Job opportunities through DKFZ's international PhD or Postdoctoral Fellowship programs (marc.kachelriess@dkfz.de).

Parts of the reconstruction software were provided by RayConStruct® GmbH, Nürnberg, Germany.